

Aquaporin 4 deficiency eliminates the beneficial effects of voluntary exercise in a mouse model of Alzheimer's disease

<https://doi.org/10.4103/1673-5374.335169>

Date of submission: May 6, 2021

Date of decision: August 7, 2021

Date of acceptance: October 12, 2021

Date of web publication: February 8, 2022

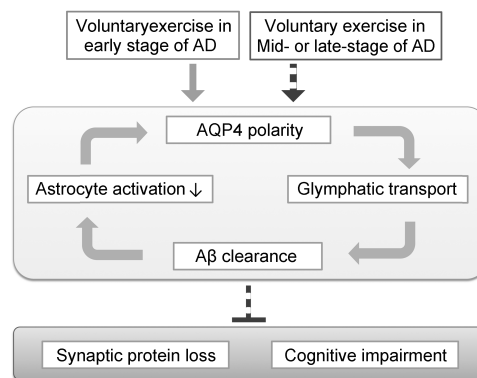
Yun Liu¹, Pan-Pan Hu^{2,3}, Shuang Zhai¹, Wei-Xi Feng^{2,3}, Rui Zhang¹, Qian Li¹, Charles Marshall⁴, Ming Xiao^{2,3,*}, Ting Wu^{1,*}

From the Contents

Introduction	2079
Materials and Methods	2080
Results	2082
Discussion	2084

Graphical Abstract

Timing-specific effects of voluntary exercise on Alzheimer's disease (AD)-like pathology



Abstract

Regular exercise has been shown to reduce the risk of Alzheimer's disease (AD). Our previous study showed that the protein aquaporin 4 (AQP4), which is specifically expressed on the paravascular processes of astrocytes, is necessary for glymphatic clearance of extracellular amyloid beta ($A\beta$) from the brain, which can delay the progression of Alzheimer's disease. However, it is not known whether AQP4-regulated glymphatic clearance of extracellular $A\beta$ is involved in beneficial effects of exercise in AD patients. Our results showed that after 2 months of voluntary wheel exercise, APP/PS1 mice that were 3 months old at the start of the intervention exhibited a decrease in $A\beta$ burden, glial activation, perivascular AQP4 mislocalization, impaired glymphatic transport, synapse protein loss, and learning and memory defects compared with mice not subjected to the exercise intervention. In contrast, APP/PS1 mice that were 7 months old at the start of the intervention exhibited impaired AQP4 polarity and reduced glymphatic clearance of extracellular $A\beta$, and the above-mentioned impairments were not alleviated after the 2-month exercise intervention. Compared with age-matched APP/PS1 mice, AQP4 knockout APP/PS1 mice had more serious defects in glymphatic function, $A\beta$ plaque deposition, and cognitive impairment, which could not be alleviated after the exercise intervention. These findings suggest that AQP4-dependent glymphatic transport is the neurobiological basis for the beneficial effects of voluntary exercises that protect against the onset of AD.

Key Words: Alzheimer's disease; amyloid-beta; astrocytes; aquaporin-4; glymphatic system; learning and memory; synaptic protein; transgenic mice; voluntary exercise

Introduction

Alzheimer's disease (AD) is a common neurodegenerative disease that is characterized by extracellular amyloid beta ($A\beta$) plaques and intracellular neurofibrillary tangles of hyperphosphorylated tau in the brain (Querfurth and LaFerla, 2010; Li et al., 2021; Manna et al., 2021). Given the lack of effective therapeutic drugs and/or vaccines for AD, non-pharmacological interventions are increasingly a research focus (Caselli et al., 2017). Results from epidemiological and interventional studies have demonstrated that regular exercise improves cognition in older adults (Richards et al., 2003; Larson et al., 2006; Zhang et al., 2018), as well as in individuals with mild cognitive

impairment (Blondell et al., 2014; Law et al., 2014, 2020). However, exercise therapy has not been shown to exert explicitly beneficial outcomes in patients with AD (Forbes et al., 2013; de Oliveira Silva et al., 2019). In several transgenic mouse models of AD, both voluntary and forced exercise has been shown to reduce extracellular brain $A\beta$ levels (Adlard et al., 2005; Xia et al., 2019; Zhang et al., 2019; Francis et al., 2020). However, there is also considerable evidence suggesting that exercise does not reduce the $A\beta$ burden in mice with mid- to late-stage AD-like pathology (Wolf et al., 2006; Ke et al., 2011; Xu et al., 2013; Robison et al., 2019). These findings indicate that the beneficial effects of exercise in promoting $A\beta$ clearance

¹Department of Neurology, the First Affiliated Hospital of Nanjing Medical University, Nanjing, Jiangsu Province, China; ²Jiangsu Province Key Laboratory of Neurodegeneration, Nanjing Medical University, Nanjing, Jiangsu Province, China; ³Brain Institute, the Affiliated Nanjing Brain Hospital of Nanjing Medical University, Nanjing, Jiangsu Province, China; ⁴College of Health Sciences, University of Kentucky Center of Excellence in Rural Health, Hazard, KY, USA

*Correspondence to: Ming Xiao, MD, PhD, mingx@njmu.edu.cn; Ting Wu, MD, PhD, wuting@njmu.edu.cn
<https://orcid.org/0000-0001-5528-9102> (Ming Xiao)

Funding: This study was supported by the National Natural Science Foundation of China, No. 81772454 (to TW) and Natural Science Foundation of Jiangsu, China, No. BK20190655 (to QL).

How to cite this article: Liu Y, Hu PP, Zhai S, Feng WX, Zhang R, Li Q, Marshall C, Xiao M, Wu T (2022) Aquaporin 4 deficiency eliminates the beneficial effects of voluntary exercise in a mouse model of Alzheimer's disease. *Neural Regen Res* 17(9):2079-2088.

may be dependent on the timing of the intervention, although the underlying mechanisms remain unclear. Imaging techniques may be particularly useful to dynamically evaluate the protective effect of aerobic exercise on glymphatic function in normal elderly individuals or those with mild cognitive impairment.

A variety of clearance pathways are implicated in the removal of A β from the brain, including enzymatic degradation, cellular uptake, and transport across the brain barriers (Tarasoff-Conway et al., 2015). Recent findings suggest that the glymphatic system may significantly contribute to extracellular A β clearance (Iliff et al., 2012). The glymphatic system, also known as the perivascular space, is surrounded by continuous incomplete astrocyte endfeet, which contain large amounts of aquaporin 4 (AQP4) (Nedergaard and Goldman, 2016). AQP4 deletion in mice impairs the glymphatic clearance of soluble macromolecular substances including A β from the brain (Iliff et al., 2012; Xu et al., 2015). A β accumulation is also linked to the loss of AQP4 polarization at the perivascular endfeet of reactive astrocytes in several models of AD, including double transgenic mice with a mutation in the Swedish amyloid precursor protein gene and the exon-9-deleted variant of the presenilin-1 gene (APPswe/PS1dE9, APP/PS1) (Xu et al., 2015; Wang et al., 2019), transgenic mice with human APP with the Arctic (E693G) and Swedish (K670N, M671L) mutations (Tg-ArcSwe) (Yang et al., 2011), and transgenic mice with five familial AD mutations (5xFAD) (Da Mesquita et al., 2018). Moreover, a recent study has shown that voluntary exercise promotes glymphatic clearance of A β in aged mice, which is associated with improved astrocyte AQP4 polarization (He et al., 2017). These results suggest that astrocyte AQP4 polarity is involved in modulating the beneficial effects of exercise interventions according to timing in AD pathology. Thus far, however, there is no direct evidence for this hypothesis.

APP/PS1 mice are extensively used as a mouse model of AD. In these mice, A β -associated long-term memory malfunctions occur from approximately 6–7 months of age, reflecting moderate-stage AD (Trinchese et al., 2004). At 3 months old, despite the absence of A β plaques, this AD mouse line exhibits mild activation of astrocytes with slight impairments of AQP4 polarity and glymphatic transport (Peng et al., 2016; Feng et al., 2020). Therefore, in the present study, we used APP/PS1 mice at 3 and 7 months old to systematically investigate the benefits of voluntary exercise on AD-like pathology according to the intervention timing. Additionally, to further explore the underlying mechanisms, we used AQP4^{-/-}/APP/PS1 mice to examine the role of AQP4 in the exercise-mediated beneficial effects in this AD model.

Materials and Methods

Animals

Compared with male littermates of the same age, AD-like pathological changes in female mice were milder, and the individual differences were more obvious. Accordingly, only male mice were used in the present study. AQP4^{-/-}/APP/PS1 mice were generated by crossing APPswe/PS1-dE9 mice (Jackson Laboratories, Philadelphia, PA, USA) with AQP4^{-/-} mice that were established in our laboratory (Fan et al., 2005), as described previously (Xu et al., 2015). We randomly divided 3- and 7-month-old male AQP4^{-/-}/APP/PS1 mice, APP/PS1 mice, and their wild-type (WT) littermates (license No. SCXK (Su) 2021-0001; Animal Core Facility of Nanjing Medical University, Nanjing, China) into exercise and sedentary groups ($n = 12-13$ per group), and then exposed those in the exercise groups to 2 months of voluntary exercise followed by behavioral testing (Figure 1A). The mice were housed 3 or 4 per cage in a room with a constant room temperature (18–22°C), a relative humidity of 30–50%, and controlled illumination (12:12 hours light/dark cycle). Food and water were available *ad libitum*. The animal experiments were approved by the Institutional Animal Care and Use Committee of Nanjing Medical University (No. IACUC-1912002) in November 2019. All experiments were designed and reported according to the Animal Research: Reporting of *In Vivo* Experiments (ARRIVE) guidelines (Percie du Sert et al., 2020).

Voluntary exercise

Mice were habituated for 1 week prior to the commencement of voluntary exercise training, referred to as the “pre-intervention” period. Each mouse in the exercise groups had free access to a 12.5 cm-diameter running wheel (Ji Biao Aquarium Co., Ltd., Jinhua, China) in a standard plastic cage (31 cm \times 22 cm \times 15 cm; Tecniplast Laboratory Equipment Trading (Shanghai) Co., Ltd., Shanghai, China) for 4 hours every day, 5 days per week, for 8 weeks (Wang et al.,

2013). For each exercise group, one mouse was randomly assigned to be placed in a cage with a modified pedometer (Pu Ning Electric Co., Ltd., Leqing, China). This enabled us to count the number of rotations during each training session (Additional Figure 1A). The running distance was calculated (rotation number \times 39.270 cm), and the average value per week was obtained (Additional Figure 1B). The control group cage was equipped with a locked running wheel, and treatment procedures were identical to those of the mice in the exercise groups. The mice were returned to their home cages after each training session.

Morris water maze test

We used the Morris water maze (MWM) task to assess spatial learning and memory function. The MWM apparatus (Beijing Sunny Instruments Co. Ltd., Beijing, China) was a black plastic pool with a diameter of 100 cm and a height of 50 cm. It was housed in a light-controlled room with surrounding distal cues and maintained at a temperature of $22 \pm 2^\circ\text{C}$. The MWM tank was divided into four quadrants, and every quadrant had a proximal cue that was a different shape, i.e., triangle, circle, square, and star. The mice received 6 days of training with a probe test on the 7th day (Xu et al., 2015). In each training trial, the mice were given up to 60 seconds to find a dark-colored cylindrical platform submerged 1 cm beneath the surface of water. The water was made opaque using milk so that the platform would be invisible to the mice, and the mice were required to remain on the platform for 5 seconds for a trial to be scored as successful. After each trial, the mice were dried and returned to their cage to rest for 15 minutes before the next trial. Mice underwent four trials per day, starting from each of the four different locations in the pool. The amount of time taken to find the hidden platform was analyzed (escape latency). During the probe trial, the platform was removed from the pool, and the mice were allowed to swim in the pool for 60 seconds. We determined the amount of time spent in the target quadrant as well as the number of times the mice crossed the location where the platform had been located.

Y-maze test

We used the Y-maze test to evaluate short-term working memory (Feng et al., 2020). We conducted two trials, separated by a 1-hour interval. The three identical arms of the maze (Beijing Sunny Instruments Co. Ltd., Beijing, China) were randomly designated as “start,” “novel,” or “other.” In the first trial, the novel arm was blocked by a removable door. The mouse was placed in the start arm and allowed to explore the two open arms for 5 minutes. In the second trial, the removable door was absent, and the mice had access to all three arms for 5 minutes. We analyzed the number of time spent in the novel arm, as well as the percentage of novel arm entries during the second trial.

Novel object recognition task

We used the novel object recognition task to assess object recognition memory (Lueptow, 2017). Mice were placed in an open field box (Beijing Sunny Instruments Co. Ltd., Beijing, China) for a 30-minute adaption period, and then subjected to two trials. During the first trial, the mice were placed in the center of the area with two identical objects and allowed to explore for 5 minutes. Following a 2-hour interval, the mice were placed back in the familiar arena, where one of the identical objects had been exchanged for a novel object. They were then allowed to freely re-explore for 5 minutes. The time spent exploring the familiar and novel objects was recorded and used to make a discrimination index where the time spent exploring the novel object was divided by the total time spent exploring both objects.

Mouse activity in the above behavioral apparatuses was recorded using a digital video camera connected to a computer-controlled system (Beijing Sunny Instruments Co. Ltd., Beijing, China). All tests were performed by authors YL and PPH, who were blind to the treatment schedule.

Cisterna magna injection with a fluorescent tracer

On the second day after behavioral testing, six mice in each group were given a cisterna magna injection with fluorescent tracer, as described previously (Iliff et al., 2012; Feng et al., 2020). The mice were anesthetized using 1% pentobarbital sodium (40 mg/kg body weight, MilliporeSigma, St. Louis, MO, USA; Cat# P-009) and fixed in a stereotaxic apparatus (Stoelting Stereotaxic Instrument, Stoelting, IL, USA) in the Trendelenburg position before surgically exposing the posterior atlanto-occipital membrane. Texas Red-dextran-3 (5 μL ; TR-d3, molecular weight: 3 kDa, Invitrogen, Carlsbad, CA,

USA, Cat# D3328) was injected at a concentration of 0.5 mg/mL into the cisterna magna (Paxinos and Franklin, 2013) via a microsyringe (Shanghai Guangzheng Medical Instrument Co. Ltd., Shanghai, China) with a flow rate of 1 μ L/min. The needle was left in place for an additional 10 minutes to prevent leakage of the tracer. Forty minutes after the start of the infusion, the animals were given an overdose of anesthetic. Their brains were then removed and post-fixed overnight in 4% paraformaldehyde at 4°C.

Tissue preparation

Following behavioral testing, the mice were intraperitoneally injected with 1% pentobarbital sodium (60 mg/kg body weight; Cat# P-009; MilliporeSigma) and perfused transcardially with 0.9% saline from the left ventricle using a perfusion pump (BT100-2J; Longer Pump, Baoding, China). The entire brain was carefully removed from the skull and divided into two hemispheres. One hemisphere was postfixed in 4% paraformaldehyde at 4°C overnight and subsequently dehydrated in a series of graded ethanol solutions. The brain tissue was embedded in paraffin and cut into 5- μ m thick sagittal sections using a sliding microtome (SM2000R; Leica, Solms, Germany). Serial sections containing the hippocampus and cerebral cortex were placed on gelatin-coated slides for immunohistochemistry, immunofluorescence, and Thioflavine-S staining. The other hemisphere was immediately frozen in liquid nitrogen and then stored at -80°C until being subjected to a Western blot or enzyme-linked immunosorbent assay (ELISA). For cerebrospinal fluid (CSF) tracer experiments, paraformaldehyde post-fixed forebrain tissues were sliced using a vibrating microtome (VT1200; Leica) at a thickness of 100 μ m, and mounted onto gelatin-coated slides in sequence.

Immunohistochemistry

Brain sections were deparaffinized, hydrated, and microwaved in citric acid buffer to achieve antigen retrieval, and then treated with 3% H₂O₂ for 20 minutes to reduce endogenous peroxidase activity. The sections were incubated with the following primary antibodies: mouse monoclonal anti-gial fibrillary acidic protein (GFAP; 1:1000; Millipore, Burlington, MA, USA; Cat# MAB360, RRID:AB_11212597), rabbit polyclonal anti-AQP4 (1:400; Millipore; Cat# AB3594, RRID:AB_91530), mouse monoclonal anti-6E10 ($\text{A}\beta_{1-16}$; 1:1000; Biolegend (Covance), San Diego, CA, USA; Cat# 803001, RRID:AB_2564653), rabbit polyclonal anti-ionized calcium binding adaptor molecule 1 (Iba1; 1:1000; Fujifilm Wako Shibayagi, Japan; Cat# 019-19741, RRID:AB_839504), rabbit polyclonal anti-postsynaptic density protein 95 (PSD95; 1:200; Abcam, Cambridge, UK; Cat# ab18258, RRID:AB_444362), and rabbit polyclonal anti-synapsin I (1:200, Abcam; Cat# ab64581, RRID:AB_1281135) at 4°C overnight. The next day, the sections were incubated for 1 hour at room temperature with horseradish peroxidase-conjugated goat anti-rabbit IgG (1:200, ZSGB-BIO, Beijing, China; Cat# ZB2301, RRID_2747412) or horseradish peroxidase-conjugated goat anti-mouse IgG antibody (1:200, ZSGB-BIO; Cat# ZB2305, RRID_2747415) and developed with a diaminobenzidine horseradish peroxidase color development kit (Millipore; Cat# DAB150). Partial AQP4 stained sections were counterstained with Congo red (MilliporeSigma; Cat# C6767).

Immunofluorescence

Brain sections were blocked for 1 hour at room temperature with 5% BSA and incubated with primary antibodies mouse monoclonal anti-GFAP (1:1000; Millipore; Cat# MAB360, RRID:AB_11212597) and rabbit polyclonal anti-AQP4 (1:400; Millipore; Cat# AB3594, RRID:AB_91530) at 4°C overnight. The next day, all sections were rinsed three times and incubated for 2 hours at room temperature in a mixture of Alexa Flour 555 donkey anti-mouse IgG (1:1000; Thermo Fisher Scientific (China) Co., Ltd., Shanghai, China; Cat# A31570, RRID:AB_2536180) and Alexa Flour 488 donkey anti-rabbit IgG (1:1000; Thermo Fisher Scientific (China) Co., Ltd.; Cat# A21206, RRID:AB_2534073). After rinsing, the sections were incubated for 6 minutes in 4',6-diamidino-2-phenylindole (1:1000; Thermo Fisher Scientific (China) Co., Ltd.; Cat# D1306) and coverslipped with anti-fluorescent quencher.

Thioflavine-S staining

Thioflavine-S staining was used to detect $\text{A}\beta$ plaques (arrowheads) in the hippocampus and adjacent cortex. Deparaffinized sections were incubated with 1% thioflavine-S (MilliporeSigma; Cat# 1326-12-1) for 5 minutes. Tissue was differentiated in 70% ethanol for 5 minutes, followed by rinsing with distilled water. The brain sections were then coverslipped with anti-fluorescent quencher.

Image analysis

Brain sections were captured using a digital microscope (DM4000B, Leica Microsystems, Wetzlar, Germany) with a constant exposure time, offset, and gain for each staining marker. The positive signal area was measured using ImageJ 1.52a (National Institutes of Health, Bethesda, MD, USA). The percentage of the area with a positive signal for GFAP, Iba1, 6E10 ($\text{A}\beta_{1-16}$), AQP4, and thioflavine-S was calculated by dividing the area with a positive signal by the total area in the hippocampus and adjacent cortex, respectively. Thioflavine-S-positive plaques and 6E10-positive plaques in the above brain regions per section were also counted. The mean integrated optical density (integrated optical density/total area) was measured to assess the immunostaining intensity of synapsin I and PSD95 in the hippocampus. To analyze AQP4 polarization, images at 400 \times magnification were randomly captured from the superficial layers of the frontal cortex (Kress et al., 2014; Xu et al., 2015). The mean immunohistochemical intensity of AQP4 at the regions immediately neighboring vessels or pia mater and adjacent parenchyma domains was measured. AQP4 polarization was calculated by comparing the expression ratios of AQP4 within perivascular domains or that abutting pia mater versus adjacent parenchymal domains (Kress et al., 2014; Xu et al., 2015). For analyzing the diffusion of intracranially injected TR-d3 into the brain parenchyma, the percentage of the area with a positive TR-d3 signal was measured on three coronal sections at +0.86, 0, and -1.06 mm from anterior to posterior, relative to bregma. TR-d3 penetration along perivascular spaces was quantified using images of the frontal cortex at 400 \times magnification. The fluorescence intensity within the perivascular space was measured along microvessels (diameter = 30–50 μ m) extending 250 μ m below the brain surface. All quantification procedures were done by investigators who were blinded regarding animal genotype and treatment.

Western blot assay

Hippocampal tissue samples were lysed in ice-cold radio immunoprecipitation assay lysis buffer (Beyotime, Shanghai, China; Cat# P0013B) containing protease inhibitors (Beyotime; Cat# st506) and phosphatase inhibitors (Roche, Basel, Switzerland; Cat# 04906837001) for 30 minutes. The homogenate was centrifuged at 12,000 $\times g$ for 15 minutes at 4°C, and the resulting supernatant fraction was collected. Protein fractions were quantitated using a bicinchoninic acid protein assay kit (Thermo Fisher Scientific (China) Co., Ltd.; Cat# 23225). Homogenous samples were loaded onto 10–12% Tris sodium dodecyl sulfate gels and transferred onto polyvinylidene fluoride membranes (Millipore). After blocking via 5% skim milk diluted with Tris-buffered saline with Tween-20 buffer for 1 hour, these membranes were incubated at 4°C overnight with one of the following primary antibodies: $\text{A}\beta_{1-40}$ (1:1000, Cat# ab20068, RRID: AB_445308, Abcam), $\text{A}\beta_{1-42}$ (1:1000, Cat# ab201060, RRID: AB_2818982, Abcam), mouse monoclonal anti-GFAP (1:1000, Cat# MAB360, RRID: AB_11212597, Millipore), rabbit polyclonal anti-Iba1 (1:1000, Cat# 019-19741, RRID: AB_839504, Fujifilm Wako, Shibayagi, Japan), rabbit polyclonal anti-synapsin I (1:1500, Cat# ab64581, RRID: AB_1281135, Abcam), rabbit polyclonal anti-PSD95 (1:1000, Cat# ab18258, RRID: AB_444362, Abcam), rabbit monoclonal anti-brain-derived neurotrophic factor (BDNF; 1:1000, Cat# Ab108319, RRID: AB_10862052, Abcam), rabbit monoclonal anti-BDNF receptor tyrosine kinase B (TrkB; 1:1000, Cat# ab187041; RRID: AB_2892613, Abcam), rabbit monoclonal anti-cAMP-response element binding protein (CREB; 1:1000, Cat# 9197S, RRID: AB_331277, CST, Danvers, MA, USA), rabbit monoclonal anti-phospho-CREB (1:1000, Cat# 9198S, RRID: AB_2561044, CST), mouse monoclonal anti- β -actin (1:500, Cat# BM0627, RRID: AB_2814866, Boster, Wuhan, China), and rabbit polyclonal anti-glyceraldehyde-3-phosphate dehydrogenase (1:3000, Cat# AF7021, RRID: AB_2839421, Affinity Biosciences, Cincinnati, OH, USA). After washing the membranes with Tris-buffered saline with Tween-20, they were incubated with horseradish peroxidase-conjugated goat anti-rabbit IgG (1:200, Cat# ZB2301, RRID: AB_2747412, ZSGB-BIO) or horseradish peroxidase-conjugated goat anti-mouse IgG (1:200, Cat# ZB2305, RRID: AB_2747415, ZSGB-BIO) for 1 hour at room temperature. The protein bands were visualized via enhanced chemiluminescence plus detection reagents (Cat# P1050-200, Applygen Technologies Inc., Beijing, China). The signal intensity of each band was quantified using ImageJ 1.52a and normalized to the corresponding loading controls, glyceraldehyde-3-phosphate dehydrogenase or β -actin.

Enzyme linked immunosorbent assay

The frontal cortex was homogenized in Tris-buffered saline with

protease inhibitors and 1% Triton X-100, followed by centrifugation at $20,000 \times g$ for 1 hour. Supernatants were set aside for measurements of soluble $A\beta_{1-40}$ (R&D Systems; Minneapolis, MN, USA; Cat# DAB140B), $A\beta_{1-42}$ (R&D Systems; Cat# DAB142), interleukin 1 beta (IL-1 β ; Excell Biotech Corporation, Shanghai, China; Cat# EM001-96), interleukin 6 (IL-6; Excell Biotech Corporation; Cat# EM004-96), or tumor necrosis factor- α (TNF- α ; Excell Biotech Corporation; Cat# EM008-96). The above indexes were quantified using the corresponding ELISA kits according to the manufacturer's instructions. The optical density of each well at 450 nm was measured using a microplate reader (Biotek Instruments, Winooski, VT, USA), and the concentrations were determined using a standard curve created by a standardized protein.

Statistical analysis

No statistical methods were used to predetermine sample sizes; however, our sample sizes are similar to those reported in previous publications (Xu et al., 2015; Feng et al., 2020). All data, expressed as mean \pm standard error of the mean (SEM), were analyzed using GraphPad Prism, version 5.02 software (GraphPad Prism Software Inc., San Diego, CA, USA). The MWM platform training data were analyzed using a three-way analysis of variance (ANOVA) with the training day, genotype, and treatment (voluntary exercise) as factors. The data regarding TR-d3 diffusion within the perivascular space were also analyzed using a three-way ANOVA with the distance from the pia surface, genotype, and treatment as factors. The other data were analyzed using a two-way ANOVA with genotype and treatment as factors. If effects were significant, further analysis was performed using Tukey's *post hoc* test for multiple comparisons. The analysis method for each dataset is indicated in the figure legends. $P < 0.05$ was considered to represent statistical significance.

Results

Deficient AQP4 eliminates the benefits of voluntary exercise on cognitive function in APP/PS1 mice

We assessed spatial learning and memory in mice using the MWM test. For the 5-month-old group, voluntary exercise reduced the escape latency in WT mice ($F_{(1, 137)} = 59.56, P < 0.0001$) and APP/PS1 mice ($F_{(1, 132)} = 39.16, P < 0.0001$), but not AQP4^{-/-}/APP/PS1 mice ($F_{(1, 134)} = 0.9870, P = 0.3223$; **Figure 1B**). For the 9-month-old group, exercise shortened the escape latency in WT mice ($F_{(1, 143)} = 36.81, P < 0.0001$), but not in APP/PS1 mice ($F_{(1, 139)} = 0.6231, P = 0.4312$) or AQP4^{-/-}/APP/PS1 mice ($F_{(1, 136)} = 0.2689, P = 0.6049$; **Figure 1C**). The time spent in the target quadrant and the number of platform crossings during the probe trials on day 7 were highest in the 5-month-old WT mice (target quadrant: $P = 0.0213$, number of platform crossings: $P = 0.02$, WT-Exe vs. WT-Con, respectively) and APP/PS1 mice in the voluntary exercise group (target quadrant: $P = 0.0429$, number of platform crossings: $P = 0.0442$, APP/PS1-Exe vs. APP/PS1-Con, respectively). For the 9-month-old group, the above parameters were only increased in the WT mice exposed to the exercise intervention (target quadrant: $P = 0.0126$; number of platform crossings: $P = 0.027$, WT-Exe vs. WT-Con, respectively). Notably, exercise did not improve spatial memory performance in the 5-month-old or 9-month-old AQP4^{-/-}/APP/PS1 mice (5-month-old: target quadrant: $P = 0.6146$, number of platform crossings: $P = 0.9853$; 9-month-old: target quadrant: $P = 0.7589$, number of platform crossings: $P = 0.9439$, AQP4^{-/-}/APP/PS1-Exe vs. AQP4^{-/-}/APP/PS1-Con, respectively; **Figure 1D and E**).

We performed the Y-maze test to measure short-term working memory. For the 5-month-old group, compared with the corresponding sedentary controls, both WT and APP/PS1 mice in the exercise group exhibited higher percentages of time spent in the novel arm ($P = 0.0225$, WT-Exe vs. WT-Con; $P = 0.0324$, APP/PS1-Exe vs. APP/PS1-Con) and a higher number of entrances into the novel arm ($P = 0.00146$, WT-Exe vs. WT-Con; $P = 0.0172$, APP/PS1-Exe vs. APP/PS1-Con). Nevertheless, the performance of the AQP4^{-/-}/APP/PS1 mice was similar between the exercise and sedentary groups (time spent: $P = 0.9174$; number of entrances: $P = 0.9610$, respectively). For the 9-month-old group, exercise increased the amount of time spent in the novel arm and the number of entrances of the WT mice (time spent: $P = 0.03$; number of entrances: $P = 0.0211$, vs. WT-Con, respectively), but failed to reverse working memory deficits in APP/PS1 mice (time spent: $P = 0.8324$; number of entrances: $P = 0.7561$, vs. APP/PS1-Con, respectively) and AQP4^{-/-}/APP/PS1 mice (time spent: $P = 0.9285$; number of entrances: $P > 0.9999$, vs. AQP4^{-/-}/APP/PS1-Con, respectively; **Figure 1F and G**).

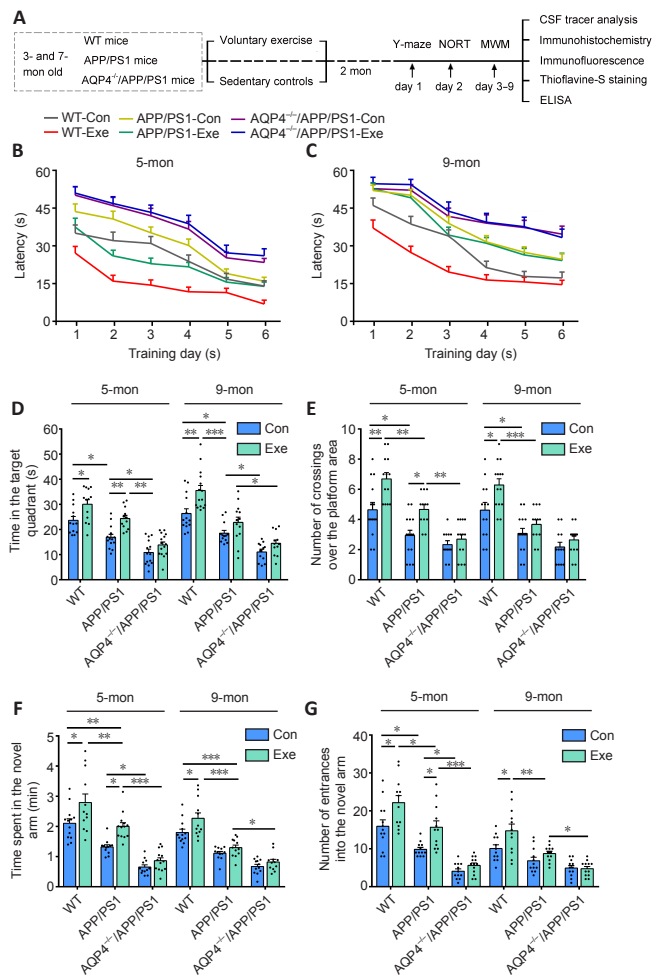


Figure 1 | Effects of voluntary exercise on cognitive function in 5- and 9-month-old APP/PS1 mice with or without AQP4.

(A) Schematic representation of the experimental design. At 3 and 7 months old, WT, APP/PS1, and AQP4^{-/-}/APP/PS1 mice were randomly assigned to voluntary exercise or sedentary groups. The mice in each group received the corresponding treatment for 2 months and then were tested using the Y-maze, NORT, and MWM followed by pathological and biochemical analyses. (B, C) The escape latency during the hidden platform training period of the MWM in the 5- (B) and 9-month-old groups (C). (D, E) The time spent in the target quadrant (D) and the number of crossings over the platform area (E) in the probe trial of the MWM. (F, G) The time spent in the novel arm (F) and number of entrances into the novel arm (G) of the Y-maze. Data represent mean \pm SEM from 12–13 mice per group. Data in B and C were analyzed using a three-way analysis of variance with Tukey's *post hoc* test, and data in D–G were analyzed using a two-way analysis of variance with Tukey's *post hoc* test. * $P < 0.05$, ** $P < 0.01$, *** $P < 0.001$. APP/PS1: Amyloid precursor protein/presenilin-1 transgenic mice; AQP4^{-/-}/APP/PS1: aquaporin 4 gene knockout and amyloid precursor protein/presenilin-1 transgenic mice; Con: sedentary group; CSF: cerebrospinal fluid; Exe: exercise group; ELISA: enzyme linked immunosorbent assay; MWM: Morris water maze; NORT: novel object recognition task; WT: wild-type mice.

We also performed the novel object recognition task to assess the effect of exercise on recognition memory in mice. For the 5-month-old group, exercise improved the discrimination index in WT and APP/PS1 mice (WT: $P = 0.0094$; APP/PS1: $P = 0.0028$, respectively) but not AQP4^{-/-}/APP/PS1 mice ($P = 0.7399$). For the 9-month group, exercise improved recognition memory in WT mice ($P = 0.0467$), but not APP/PS1 mice ($P = 0.9934$) or AQP4^{-/-}/APP/PS1 mice ($P = 0.7073$; **Additional Figure 2**). Together, these behavioral results demonstrate that voluntary exercise has a beneficial effect on cognition in the early stage but not the middle stage of the APP/PS1 mouse model of AD, and that this improvement does not occur when the mice have an absence of AQP4.

AQP4 deficiency abolishes the beneficial effect of voluntary exercise on glymphatic transport in APP/PS1 mice

We assessed glymphatic transport by quantifying TR-d3 penetration into the brain parenchyma following a cisterna magna injection

(Figure 2A). We found that APP/PS1 mice had a smaller percentage of the TR-d3-positive area and a decreased paravascular fluorescence intensity compared with WT mice at the age of 5 months (area percentage: $P = 0.0042$; fluorescence intensity: $F_{(1, 29)} = 42.98$, $P < 0.0001$) and 9 months (area percentage: $P = 0.0022$; fluorescence intensity: $F_{(1, 30)} = 91.07$, $P < 0.0001$, respectively). Both 5- and 9-month-old WT mice exposed to voluntary exercise exhibited an increased fluorescence penetration area (5 months: $P = 0.0022$; 9 months: $P = 0.0029$, vs. control, respectively) and an increased intensity (5 months: $F_{(1, 28)} = 39.05$, $P < 0.0001$; 9 months: $F_{(1, 30)} = 21.12$, $P < 0.0001$, vs. control, respectively). However, for APP/PS1 mice, the beneficial effect of exercise on penetration of TR-

d3 into the brain parenchyma was observed in the 5-month group only (area percentage: $P = 0.0033$; fluorescence intensity: $F_{(1, 29)} = 39.27$, $P < 0.0001$, vs. control, respectively). Neither 5- nor 9-month-old AQP4^{-/-}/APP/PS1 mice treated with exercise showed an increase in the percentage of the TR-d3 positive area (5 months: $P = 0.8651$; 9 months: $P = 0.9786$) or the paravascular fluorescence intensity (5 months: $F_{(1, 30)} = 0.3178$, $P = 0.5771$; 9 months: $F_{(1, 30)} = 1.693$, $P = 0.2031$; Figure 2B–F and Additional Figure 3). These results suggest that the ameliorating effect of exercise on glymphatic transport malfunction in APP/PS1 mice is timing-dependent, and that AQP4 deletion eliminates the beneficial effect of exercise on glymphatic transport.

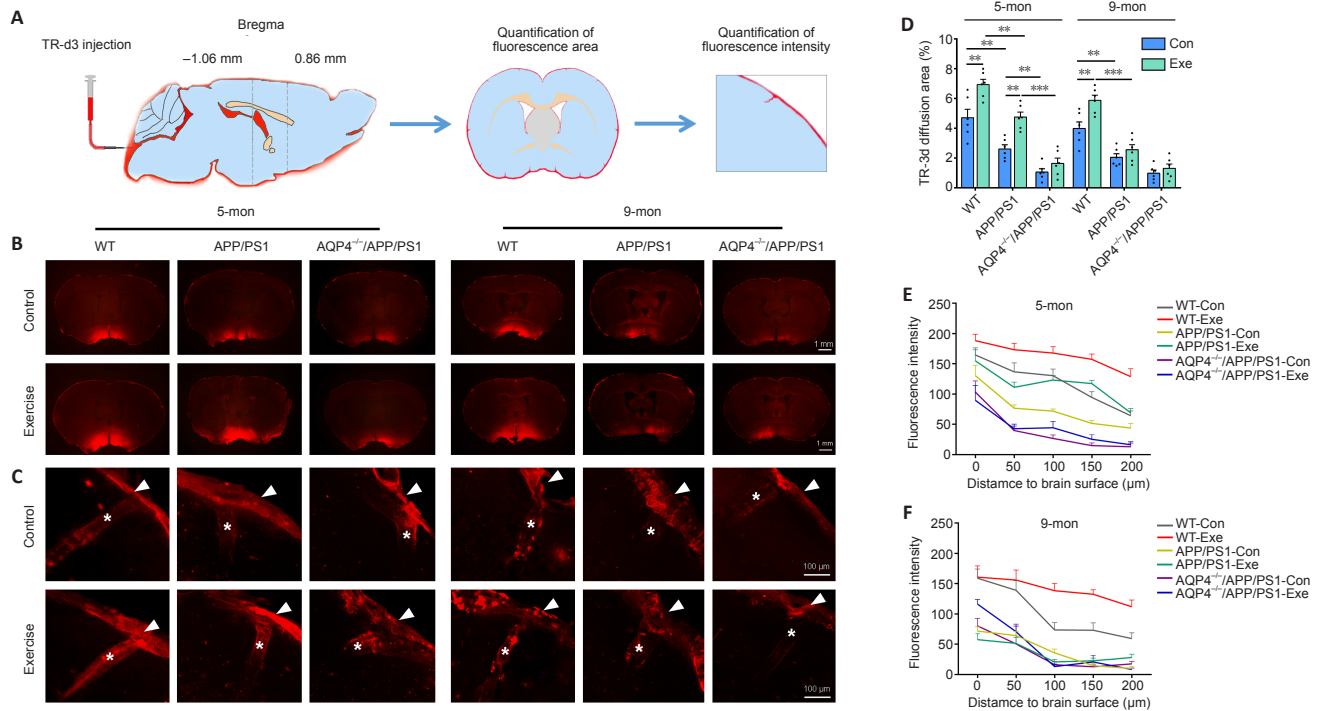


Figure 2 | Effect of voluntary exercise on glymphatic transport in 5- and 9-month-old APP/PS1 mice with or without AQP4. (A) Schematic diagram showing intracisternal injection of TR-d3 tracer and experiment schedule. (B) Representative images of coronal brain sections of each group at bregma 0 mm showing the TR-d3 influx into the brain at 40 minutes after the cisterna magna injection. (C) High magnification micrographs of the frontal cortex showing TR-d3 distribution on the brain surface (arrowheads) and within the perivascular space (stars). Exercise improved the penetration of TR-d3 into the brain parenchyma in the 5- and 9-month-old WT mice and 5-month-old APP/PS1 mice, but not in the 9-month-old APP/PS1 mice or 5- and 9-month-old AQP4^{-/-}/APP/PS1 mice. Scale bars: 1 mm in B, 100 μm in C. (D) Quantification of the area percentage of TR-d3 fluorescence in the brain section. (E, F) Quantification of the mean fluorescence intensity of TR-d3 along the perivascular space in the 5- (E) and 9-month-old groups (F), respectively. Data represent mean ± SEM from 4 sections (in D) or 6–8 microvessels (in E and F) per mouse, with 6 mice per group. Data in D were analyzed using a two-way factor analysis of variance with Tukey's *post hoc* test. Data in E and F were analyzed using a three-way analysis of variance with Tukey's *post hoc* test. ** $P < 0.01$, *** $P < 0.001$. APP/PS1: Amyloid precursor protein/presenilin-1 transgenic mice; AQP4^{-/-}/APP/PS1: aquaporin 4 gene knockout and amyloid precursor protein/presenilin-1 transgenic mice; Con: sedentary group; Exe: exercise group; TR-d3: Texas red-dextran-3; WT: wild-type mice.

AQP4 deficiency negates the reduction in brain Aβ load induced by voluntary exercise in APP/PS1 mice

We further evaluated whether voluntary exercise offered at different time points had unique effects on the reduction of the brain Aβ burden in APP/PS1 mice. Compared with age-matched APP/PS1 mice, both 5- and 9-month-old AQP4^{-/-}/APP/PS1 mice showed an increased Aβ load in the hippocampus and frontal cortex, as revealed by quantification of the area percentage and number of thioflavine-S positive fibrillar plaques and 6E10-immunopositive diffuse plaques (all $P < 0.05$). Exercise decreased Aβ plaque accumulation in the above two brain regions in APP/PS1 mice at 5 months (all $P < 0.05$ for the above indexes). We did not observe a beneficial effect of exercise on Aβ load in the AQP4^{-/-}/APP/PS1 mice at either of the two different time points (all $P > 0.05$; Figure 3A–F). Consistent with this, the Western blot and ELISA revealed that voluntary exercise only decreased Aβ_{1–40} and Aβ_{1–42} levels in the forebrain samples of 5-month-old APP/PS1 mice (all $P < 0.05$) rather than the 9-month-old APP/PS1 mice (all $P > 0.05$). Voluntary exercise failed to decrease brain Aβ_{1–40} and Aβ_{1–42} levels in both 5- and 9-month-old AQP4^{-/-}/APP/PS1 mice (all $P > 0.05$; Figure 3G–I and Additional Figure 4A and B). The above data indicate that voluntary exercise reduces brain Aβ load in APP/PS1 mice in a timing-dependent manner, and that this effect is reliant on the presence of AQP4.

AQP4 deficiency dampens the ameliorating effect of voluntary exercise on reactive gliosis and neuroinflammation in APP/PS1 mice

In addition to Aβ deposition, reactive gliosis is a pathological hallmark of AD (Lopategui Cabezas et al., 2014; Acosta et al., 2017). We determined the effects of voluntary exercise and/or AQP4 deletion on the activation of astrocytes and microglia in APP/PS1 mice at different stages of AD-like progression. Both GFAP-positive astrocytes and Iba1-positive microglia were activated in the frontal cortex and hippocampus of APP/PS1 mice at 5 months old, and this was increasingly apparent at 9 months old. AQP4 deletion in 5-month-old APP/PS1 mice mildly increased the activation of microglia and astrocytes in the frontal cortex and hippocampus. Microglia activation was also more pronounced in AQP4^{-/-}/APP/PS1 mice at 9 months, as revealed by the high percentages of Iba1 positive areas in the frontal cortex ($P = 0.0011$) and hippocampus ($P = 0.0168$) compared with that in age-matched APP/PS1 mice. However, a considerable proportion of astrocytes underwent atrophy, characterized by a breakdown of the cell body with residual processes, in 9-month-old AQP4^{-/-}/APP/PS1 mice (Figure 4A and Additional Figure 5A). There was no overall change in immunohistochemical labeling patterns of GFAP or Iba1 in the frontal cortex and hippocampus in 5- and 9-month-old WT-exercise mice compared with that in

age-matched sedentary controls. As for APP/PS1 mice, exercise reduced the percentages of the positive areas for GFAP (cortex: $P = 0.0416$; hippocampus: $P = 0.0331$) and Iba1 (cortex: $P = 0.0027$; hippocampus: $P = 0.0107$) in the 5-month-old group but not the 9-month-old group (GFAP: cortex, $P = 0.9704$; hippocampus, $P = 0.9993$; Iba-1: cortex, $P = 0.9887$; hippocampus, $P > 0.9999$). Exercise did not mitigate the reactivation of astrocytes or microglia in AQP4^{-/-}/APP/PS1 mice in either age group (5 months: GFAP: cortex, $P = 0.9991$; hippocampus, $P = 0.3894$; Iba-1: cortex, $P > 0.9999$; hippocampus, $P = 0.9745$; 9 months: GFAP: cortex, $P = 0.5592$; hippocampus, $P = 0.9685$; Iba-1: cortex, $P = 0.9579$; hippocampus, $P = 0.9994$; **Figure 4B and C** and **Additional Figure 5B**). The Western blot results also showed that the AQP4 deficiency eliminated the time-dependent effects of voluntary exercise on GFAP and Iba1 expression levels in the hippocampus of APP/PS1 mice (5 months: GFAP: $P = 0.9986$; Iba-1: $P = 0.9931$; 9 months: GFAP: $P > 0.9999$; Iba-1: $P = 0.9602$; **Figure 4D–F**). Consistent with this, voluntary exercise partially reduced neuroinflammatory factor levels in APP/PS1 mice at 5 months (IL-1 β : $P = 0.0121$; IL-6: $P = 0.0184$; TNF- α : $P = 0.0191$), but not at 9 months old (IL-1 β : $P = 0.9883$; IL-6: $P > 0.9999$; TNF- α : $P = 0.9964$). The AQP4 deletion in APP/PS1 mice completely abolished the mitigating effect of the exercise intervention on neuroinflammation (5 months: IL-1 β : $P = 0.8353$; IL-6: $P = 0.7361$; TNF- α : $P = 0.9959$; 9 months: IL-1 β : $P = 0.9966$; IL-6: $P = 0.7856$; TNF- α : $P = 0.9983$; **Additional Figure 5C**). The above results indicate that voluntary exercise ameliorates reactive gliosis and neuroinflammation in the onset stage but not the mid-stage of APP/PS1 mice, and that this timing effect is absent in AQP4^{-/-}/APP/PS1 mice.

Voluntary exercise ameliorates impaired polarization of astrocyte AQP4 in the onset stage but not mid-stage in APP/PS1 mice

Substantial evidence suggests that reactive astrogliosis results in the mislocalization of AQP4 from the endfeet to the entire cell surface of astrocytes, subsequently contributing to dysfunctional glymphatic clearance (Iliff et al., 2012; Kress et al., 2014; Wang et al., 2019). Here, immunohistochemical staining revealed that AQP4 expression selectively bordered the subarachnoid space and microvessels with very low intensity in the adjacent brain parenchyma in WT mice. AQP4 was abnormally expressed at the non-vascular domains, especially those surrounding Congo-red positive plaques, in 5-month-old APP/PS1 mice (**Figure 5A**). The mislocalization of AQP4 was further discernible in the brain parenchyma of 9-month-old APP/PS1 mice, causing a total loss of AQP4 polarity. Voluntary exercise decreased AQP4 expression at the non-vascular domains in 5-month-old APP/PS1 mice but not 9-month-old APP/PS1 mice. Semi-quantitative analysis demonstrated that voluntary exercise decreased the percentage of the AQP4-positive area ($P = 0.0078$) and improved AQP4 polarity around microvessels ($P = 0.0398$) and pia mater ($P = 0.0148$) in 5-month-old APP/PS1 mice exposed to exercise. In contrast, these changes were not apparent in 9-month-old APP/PS1 mice exposed to exercise (percentage of the AQP4-positive area: $P = 0.8609$; AQP4 polarization around microvessels: $P = 0.9586$; AQP4 polarization around pia surface: $P = 0.0944$; **Figure 5B–D**). Double immunofluorescence labeling for GFAP and AQP4 further confirmed the presence of activated astrocytes with impaired AQP4 polarization in the brain parenchyma of both 5- and 9-month-old APP/PS1 mice, indicating that voluntary exercise ameliorated the mislocalization of astrocyte AQP4 in the onset stage but not mid-stage of progression in APP/PS1 mice (**Additional Figure 6A and B**).

AQP4 deficiency eliminates the beneficial effect of voluntary exercise on the expression levels of proteins related to the BDNF signaling pathway and synaptic plasticity in APP/PS1 mice

The BDNF signaling pathway is associated with synaptic function and regulates the expression of synaptic proteins (Poo, 2001; Chao, 2003). Down-regulation of the BDNF signaling pathway and synaptic protein loss occur in AD patients (Peng et al., 2005; Kim et al., 2017) as well as animal models of AD (Poon et al., 2011; Bartolotti et al., 2016). Moreover, the BDNF signaling pathway is involved in the neuroprotective effects of exercise in AD (Vaynman et al., 2004; Liu and Nusslock, 2018), stroke (Ferrer et al., 2001; Liu et al., 2020), and depression (Duman and Monteggia, 2006; Martinowich et al., 2007). The present study measured the activation of the BDNF-TrkB-CREB pathway and the expression levels of PSD95 and synapsin I in the forebrain. We found that the expression levels of BDNF (mature form), TrkB, and p-CREB generally decreased in APP/PS1 mice compared with those in WT controls at 5 (BDNF: $P < 0.0001$; TrkB: $P = 0.0004$; p-CREB: $P = 0.0002$, respectively) and 9 months old (BDNF: $P < 0.0001$; TrkB: $P = 0.6340$; p-CREB: $P = 0.0014$,

respectively). Voluntary exercise activated this signaling pathway in WT mice aged 5 (BDNF: $P = 0.0001$; TrkB: $P = 0.4700$; p-CREB: $P = 0.0002$, respectively) and 9 months old (BDNF: $P < 0.0001$; TrkB: $P < 0.0001$; p-CREB: $P < 0.0001$, respectively), but this was only the case in APP/PS1 mice at 5 months old (BDNF: $P < 0.0001$; TrkB: $P = 0.0090$; p-CREB: $P = 0.0329$, respectively; **Figure 6A and B**). Consistent with this, voluntary exercise significantly up-regulated synapsin I and PSD95 levels in the hippocampus of 5-month-old WT and APP/PS1 mice (all $P < 0.05$), but not AQP4^{-/-}/APP/PS1 mice (all $P > 0.05$), as revealed by immunohistochemical staining and Western blot analysis. For the 9-month-old group, a beneficial effect of voluntary exercise on synaptic protein levels was only observed in WT mice (immunohistochemistry: synapsin I: $P = 0.0146$; PSD95: $P = 0.0494$; Western blot: synapsin I: $P < 0.0001$; PSD95: $P = 0.0309$, respectively; **Figure 6C and D** and **Additional Figure 7A–C**). Together, these results indicate that voluntary exercise improves BDNF signaling activation and synaptic plasticity in the hippocampus of APP/PS1 mice in a timing-dependent manner, which is eliminated in the absence of AQP4.

Discussion

Epidemiological evidence suggests that regular exercise may reduce the risk or delay the onset of AD, yet clinical trials demonstrate no cognitive benefits of exercise therapy in patients with AD (Forbes et al., 2013; Blondell et al., 2014; Law et al., 2014, 2020; Zhang et al., 2018; de Oliveira Silva et al., 2019). The current study was designed to address the underlying mechanisms of exercise in mitigating A β -related pathology and cognitive dysfunction in APP/PS1 mice. The results show that APP/PS1 mice with access to voluntary exercise exhibit different effects depending on how old they were during the exercise. The early exercise intervention improved AQP4 polarization at the perivascular endfeet of astrocytes in the brains of 5-month-old APP/PS1 mice, subsequently promoting glymphatic transport and reducing brain A β load. This in turn decreased glial activation, inflammatory factor production, and alterations of synapse-related signaling pathways. However, during the mid-stage of AD-like pathology, AQP4 polarity is disrupted because of reactive astrogliosis (Iliff et al., 2014; Kress et al., 2014). Therefore, the structural basis for the beneficial effect of exercise on glymphatic clearance is damaged, which subsequently leads to a failure to prevent A β -related pathological cascades. In addition, 5- and 9-month-old AQP4^{-/-}/APP/PS1 mice showed more severe glymphatic malfunction, A β burden, and cognitive defects compared with age-matched APP/PS1 mice. Voluntary exercise had no beneficial effects on AQP4^{-/-}/APP/PS1 mice, further suggesting that AQP4 may be a critical therapeutic target for the potential use of exercise to delay the onset of AD.

Increasing evidence supports the idea that the glymphatic system plays a central role in the clearance of macromolecular substances from the brain (Nedergaard and Goldman, 2016). The notion of this clearance mechanism has opened up new perspectives in understanding the pathogenesis of AD (Valenza et al., 2019; Reeves et al., 2020), stroke (Goulay et al., 2020; Mestre et al., 2020), brain injury (Piantino et al., 2019), and other neurological diseases (Rasmussen et al., 2018; Nikolenko et al., 2020). It suggests that the AQP4-mediated rapid transport of intercellular water is a main “driving force” for glymphatic clearance of interstitial solutes from the brain parenchyma into the blood and CSF (Mestre et al., 2018). In an AQP4 gene knockout, the clearance of exogenous A β from the brains of mice following an intrastriatal injection was significantly delayed (Iliff et al., 2012). Our present and previous studies consistently demonstrate that AQP4 deletion in APP/PS1 mice exacerbates impaired glymphatic clearance and A β accumulation (Xu et al., 2015; Feng et al., 2020).

The current results further support the view that glymphatic clearance not only depends on the presence of AQP4, but also on its specific localization at perivascular astrocyte endfeet and astrocyte processes of the glial limitans (Iliff et al., 2012; Kress et al., 2014). This distribution pattern of AQP4 facilitates the influx of subarachnoid CSF from para-arterial spaces into the brain interstitium, as well as the subsequent clearance of interstitial fluid (ISF) via convective bulk flow (Nedergaard and Goldman, 2016; Rasmussen et al., 2018). Reactive astrogliosis, a feature of the aging brain and one of the hallmarks of AD (Lopategui Cabezas et al., 2014; Acosta et al., 2017), results in the loss of perivascular AQP4 polarization (Iliff et al., 2014; Kress et al., 2014). AQP4 relocalizes from the perivascular feet to the soma, and nonperivascular astrocyte processes hamper the clearance of brain waste. The loss of perivascular AQP4 polarization

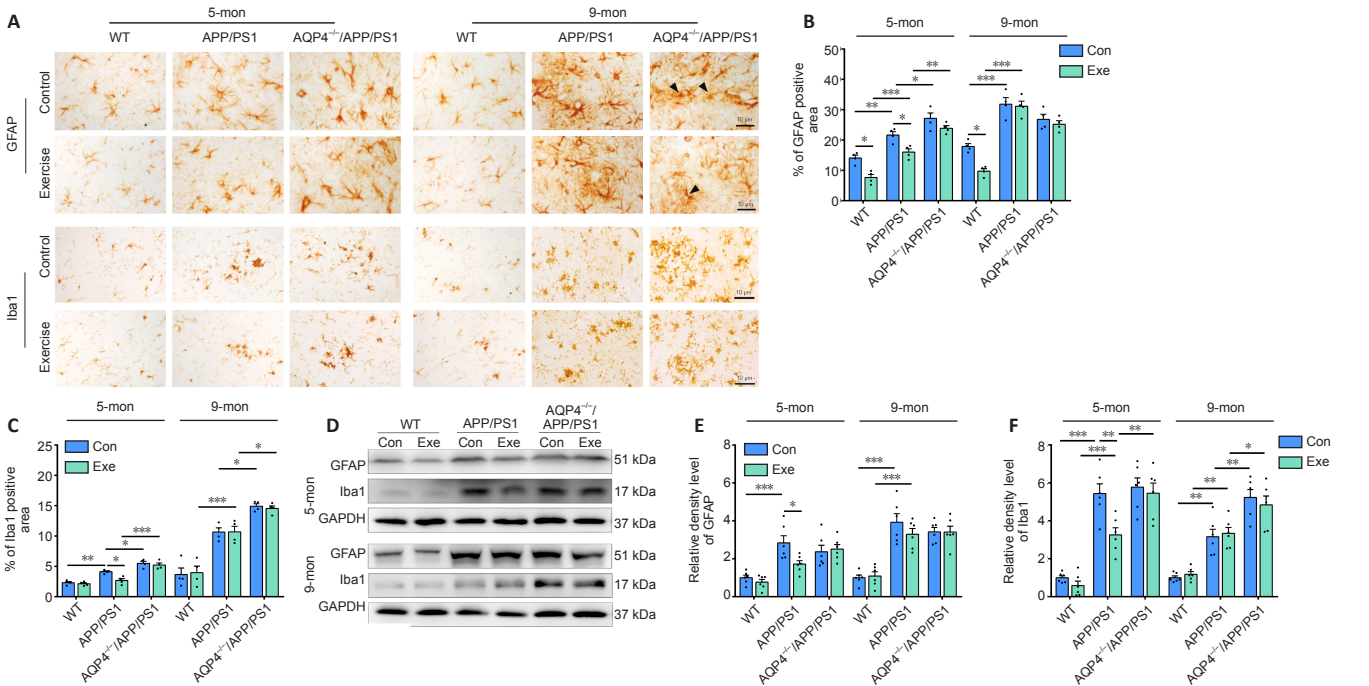
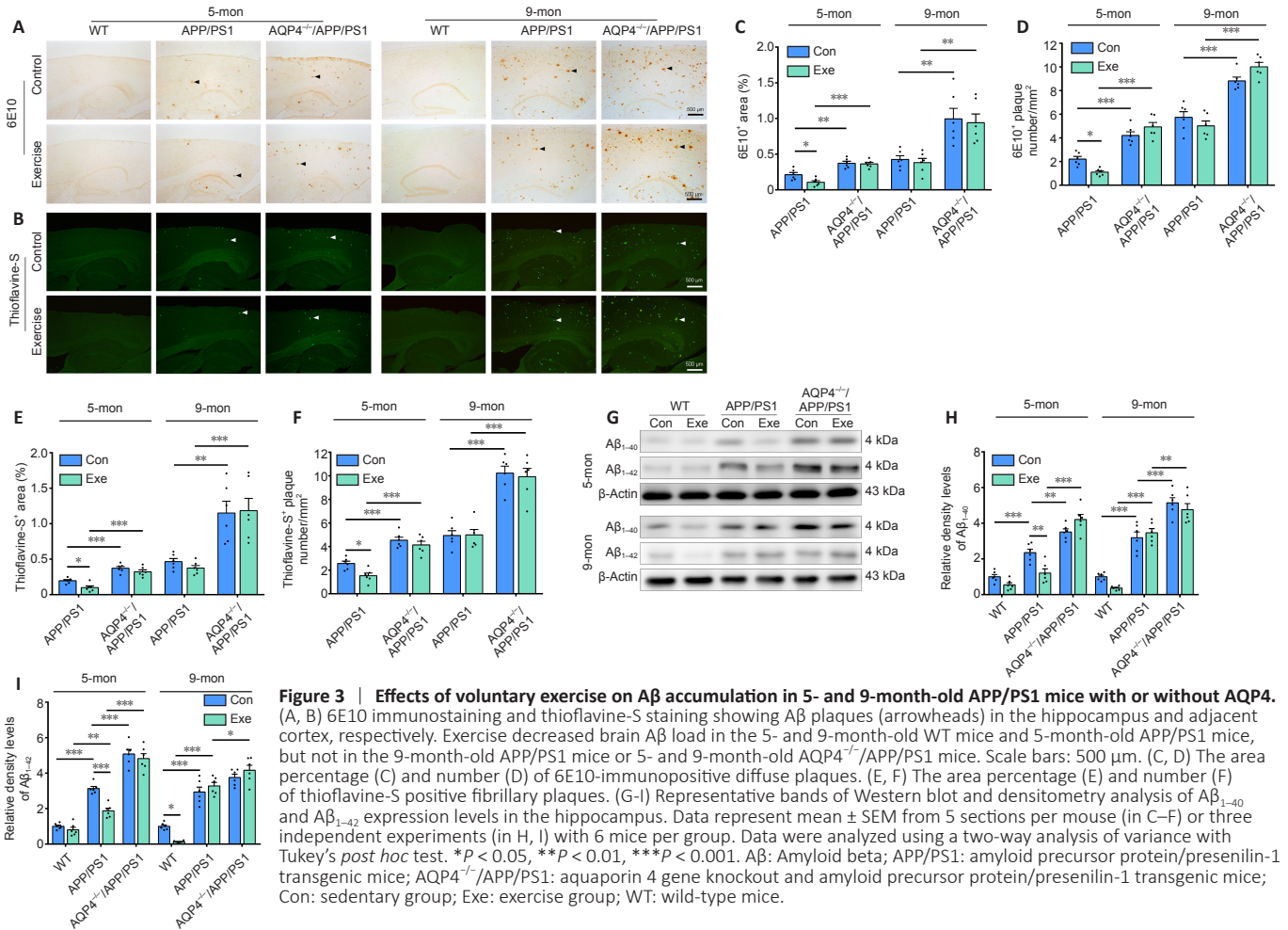


Figure 5 | Effects of voluntary exercise on AQP4 expression and polarity in the frontal cortex in 5- and 9-month-old APP/PS1 mice as revealed by AQP4 and Congo-red double staining.

(A) Representative AQP4 immunoreactive images of the frontal cortex show localization of AQP4 abutting the pia mater (black arrowheads) and microvessels (grey arrowheads). Note that AQP4 is expressed at parenchymal domains surrounding A β plaques (white arrowheads). Exercise attenuated the mislocalization of AQP4 in the brain parenchyma of 5-month-old APP/PS1 mice, but not 9-month-old APP/PS1 mice. Scale bars: 50 μ m. (B) The percentage of the AQP4-positive area in the frontal cortex. (C) The polarization of AQP4 abutting the pia surface. (D) The polarization of AQP4 around microvessels. Data are represented as mean \pm SEM from four sections (16–20 microvessels) per mouse with four mice per group and were analyzed using a two-way analysis of variance with Tukey's *post hoc* test. * $P < 0.05$, ** $P < 0.01$, *** $P < 0.001$. APP/PS1: Amyloid precursor protein/presenilin-1 transgenic mice; AQP4^{-/-}/APP/PS1: aquaporin 4 gene knockout and amyloid precursor protein/presenilin-1 transgenic mice; Con: sedentary group; Exe: exercise group; WT: wild-type mice.

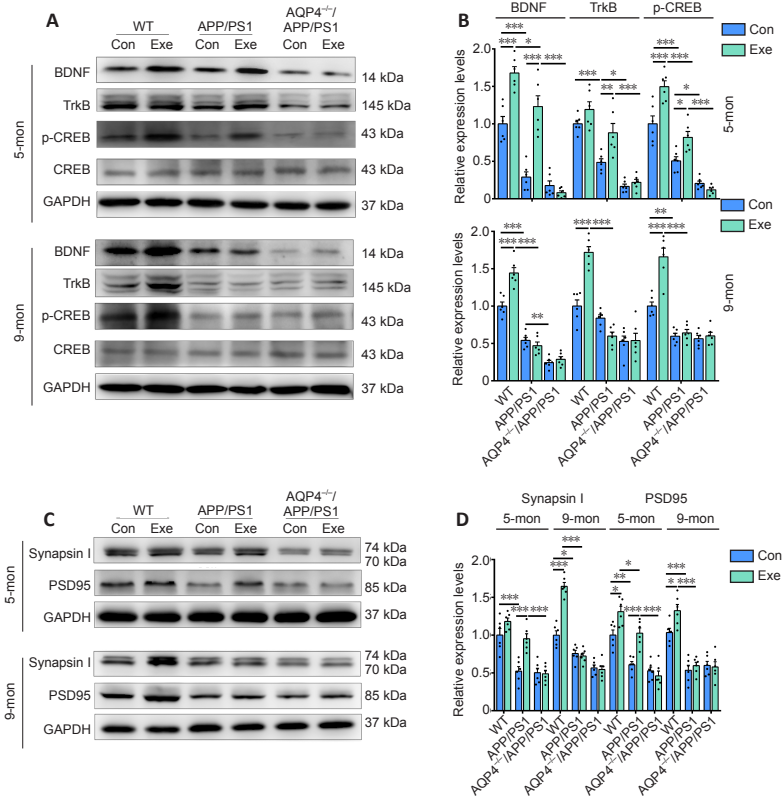
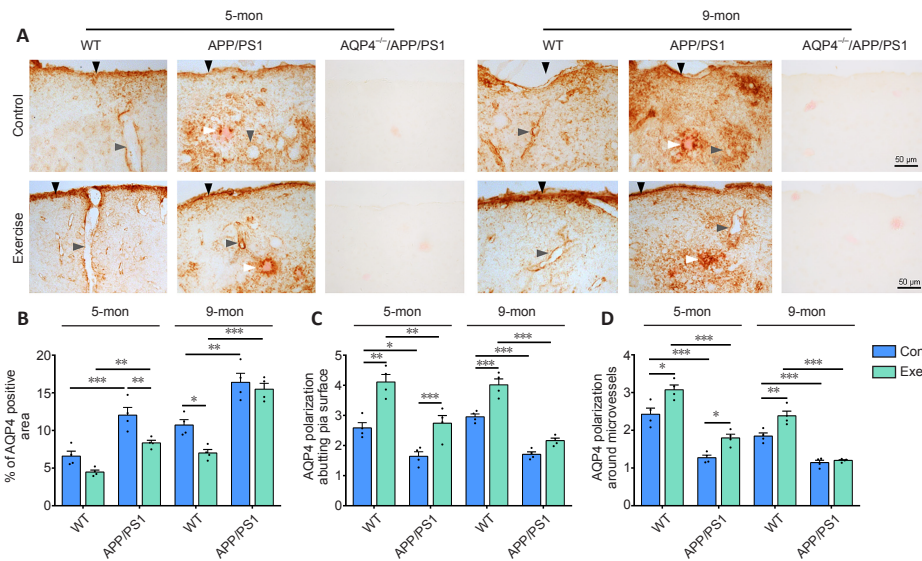


Figure 6 | Effects of voluntary exercise on BDNF-TrkB signaling activation and synaptic protein levels in the hippocampus of 5- and 9-month-old APP/PS1 mice with or without AQP4.

(A, B) Representative bands of Western blot and densitometry analysis of BDNF, TrkB, and p-CREB levels. (C, D) Representative bands of Western blot and densitometry analysis of synapsin I and PSD95 expression levels in the hippocampus. Data represent mean \pm SEM from three independent experiments with six mice per group, and were analyzed using a two-way analysis of variance with Tukey's *post hoc* test. * $P < 0.05$, ** $P < 0.01$, *** $P < 0.001$. APP/PS1: Amyloid precursor protein/presenilin-1 transgenic mice; AQP4^{-/-}/APP/PS1: aquaporin 4 gene knockout and amyloid precursor protein/presenilin-1 transgenic mice; BDNF: brain-derived neurotrophic factor; Con: sedentary group; CREB: CAMP-response element binding protein; Exe: exercise group; GAPDH: glyceraldehyde-3-phosphate dehydrogenase; p-CREB: phospho-CREB; PSD95: postsynaptic density protein 95; TrkB: BDNF receptor tyrosine kinase B; WT: wild-type mice

is associated with glymphatic pathway impairment, which has been demonstrated in aged mice (Kress et al., 2014) and mouse models of AD (Yang et al., 2011; Xu et al., 2015; Da Mesquita et al., 2018; Wang et al., 2019). These results imply that specific expression of AQP4 on the perivascular endfeet of astrocytes is necessary for glymphatic system-mediated bulk flow of ISF.

Consistent with the results of animal experiments, alterations in AQP4 expression and localization in the fronto-temporal lobe are associated with AD status and pathology, which is related to noncoding Aqp4 single-nucleotide polymorphisms (Burfeind et al., 2017; Zeppenfeld et al., 2017). Notably, perivascular AQP4 localization is preserved among individuals older than 85 years who remain cognitively intact. The loss of perivascular AQP4 localization

is associated with increased A β deposition (Burfeind et al., 2017; Zeppenfeld et al., 2017). Assessments of perivascular fluid movement via diffusion tensor magnetic resonance imaging have indicated that lymphatic transport ability is lower in AD patients than in healthy controls of the same age (Taoka et al., 2017). Together, the results from both animal and human studies indicate that AQP4 is vital for glymphatic clearance, thus playing a critical role in regulating the pathological progress of AD. AQP4 has broad tissue distribution and is involved in a variety of cellular and organ functions. Therefore, there are a series of challenges for the establishment of AQP4-target therapeutics in protecting against the onset of AD. Further studies are needed to examine the efficacy of AQP4 modulators in protecting glymphatic function in transgenic mouse models of AD.



Evidence from recent studies strongly indicates that glymphatic clearance mediates the neuroprotective effects of voluntary exercise. Voluntary exercise has been shown to increase cerebral arterial pulsation and enhance paravascular CSF-ISF exchange in young, freely behaving, and awake mice (von Holstein-Rathlou et al., 2018). Moreover, aged mice taking part in voluntary exercise exhibit decreased astrocyte activation, improved AQP4 polarity and glymphatic transport, and low brain A β concentration compared with sedentary controls (He et al., 2017). Consistent with this, the present results confirm that in the onset stage of AD-like pathology in APP/PS1 mice, voluntary exercise attenuates reactive astrogliosis and the mislocalization of AQP4 at the nonperivascular processes of astrocytes, subsequently reducing A β plaque accumulation. However, in the mid-stage of progression in APP/PS1 mice, there is prominent A β plaque deposition in the brain parenchyma, accompanied by extensive activation of astrocytes and mislocalization of AQP4 (Xu et al., 2015; Peng et al., 2016). In this case, the increased cerebral perfusion induced by exercise may result in ISF turbulence, which may inhibit the removal of A β from the brain parenchyma through the paravenous approach. This conclusion is supported by nonsignificant increases in A β 1-40 levels in the hippocampus of 9-month-old APP/PS1 mice that received voluntary exercise for 2 months.

In agreement with the present findings, previous studies have reported an age-dependent beneficial effect of a continuous non-shock treadmill exercise paradigm on the pathogenic characteristics of APP/PS1 transgenic mice. Five weeks of exercise reduced A β 1-40 and A β 1-42 levels in the hippocampus of adult (7–8-month-old) APP/PS1 mice, but not aged (24-month-old) APP/PS1 mice. Furthermore, exercise did not reduce plaque loading in either adult or aged APP/PS1 mice (Ke et al., 2011). In contrast, a 4-month treadmill exercise intervention significantly improved spatial learning and memory ability, reduced amyloid plaques in the hippocampus, and induced neurogenesis in the dentate gyrus of 12-month-old APP/PS1 mice (Chao et al., 2018). This indicates that a longer exercise intervention period may have a more beneficial effect in delaying the pathological progression in AD mice. In addition, exercise at different intensities may have varying effects on APP/PS1 mice. Moderate exercise intensity (60–70% of max oxygen uptake) seems to be more effective in increasing lipid metabolism and reducing soluble A β levels compared with low-intensity exercise (45–55% of max oxygen uptake) (Zeng et al., 2020). Future studies are needed to clarify the effects of exercise intensity and duration on glymphatic clearance. Particularly, non-invasive imaging techniques are valuable for dynamically evaluating the protective effect of aerobic exercise on glymphatic function in normal elderly individuals or those with mild cognitive impairment.

One limitation of the current study is that AQP4^{-/-} mice were not included. This was to reduce the number of animal groups. Previous studies, including those from our laboratory, have revealed that an AQP4 deficiency does not change brain A β levels under baseline conditions. AQP4^{-/-} mice have normal expression levels of enzymes and proteins related to A β production and degradation, as well as an intact meningeal lymphatic draining pathway (Ilfiff et al., 2012; Xu et al., 2015; Mestre et al., 2018; Feng et al., 2020). However, exercise plays a variety of neuroprotective roles, including promoting neurogenesis, reducing neuroinflammation, improving mitochondrial energy metabolism, and promoting neurotrophic factor secretion (Jahangiri et al., 2019; Quan et al., 2020). Thus, the effect of voluntary exercise on AQP4^{-/-} mice remains unclear, and further research is needed. Further research is also needed to determine whether the over-expression of AQP4 or enhanced AQP4 polarity could enhance neuroprotection induced by aerobic exercise.

In addition to AQP4, human astrocytes increase the expression of AQP1 under various pathological conditions such as cerebral infarction (Sato et al., 2007), multiple sclerosis (Sato et al., 2007), Gerstmann-Sträussler-Scheinker disease (Sadashima et al., 2020), Creutzfeldt-Jakob disease (Rodríguez et al., 2006), Parkinson's disease (Hoshi et al., 2017), and AD (Pérez et al., 2007; Hoshi et al., 2012). AQP1-expressing fibrillary astrocytes are closely associated with A β plaques in the brains of AD patients (Misawa et al., 2008) and prion plaques in patients with Gerstmann-Sträussler-Scheinker disease (Sadashima et al., 2020), suggesting an involvement in plaque formation. Neuronal AQP1 accumulation is also observed in the brains of AD patients as well as 3xTg-AD and 5xFAD mice (Park et al., 2021). Upregulated AQP1 in neurons may inhibit A β production by reducing the interaction between APP and β -secretase (Park et al.,

2021). Previous studies have revealed increased expression of AQP4, but not AQP1, in subpial and subependymal regions as well as around blood vessels in the brains of AD patients (Moftakhar et al., 2010). These data suggest that an upregulation of AQP1 might contribute to the inhibition of brain A β production, while mislocalization of AQP4 might hinder glymphatic clearance of A β during AD progression. Further studies are required to determine whether AQP1 is involved in the timing-dependent effects of voluntary exercise on AD pathology.

In conclusion, this study revealed that long-term voluntary exercise promotes the removal of A β , attenuating its aggregation, and subsequently reducing astrocyte activation, which is conducive to the maintenance of AQP4 polarity. This effect, in turn, maintains glymphatic transport capability, thereby effectively improving cognitive function in adult WT mice and delaying the onset of AD-like pathogenesis in APP/PS1 mice. However, a voluntary exercise intervention failed to enhance A β clearance and alleviate AD-like pathology under the condition of AQP4 deficiency or AQP4 polarity damage. These results reveal that astrocyte AQP4 mediates the beneficial effect of voluntary exercise on A β -related pathology, potentially offering a new target for the early prevention of AD. Furthermore, our findings regarding the molecular pathological mechanisms of AD explain why exercise might help to prevent AD, but not cure AD, which has been a long-standing dilemma in the field of AD research.

Author contributions: Study design: TW; experiment implementation and statistical analysis: YL, WXF, RZ, PPH, SZ; data interpretation: YL, WXF, QL; manuscript writing: YL, MX; manuscript revision: CM. All authors read and approved the final version of the manuscript.

Conflicts of interest: The authors declare no conflict of interests.

Author statement: This paper has been posted as a preprint on Research Square with doi: <https://doi.org/10.21203/rs.3.rs-108136/v1>, which is available from: <https://assets.researchsquare.com/files/rs-108136/v1/623738f2-c684-4caa-81f8-88f71ee93286.pdf>.

Availability of data and materials: All data generated or analyzed during this study are included in this published article and its supplementary information files.

Open access statement: This is an open access journal, and articles are distributed under the terms of the Creative Commons AttributionNonCommercial-ShareAlike 4.0 License, which allows others to remix, tweak, and build upon the work non-commercially, as long as appropriate credit is given and the new creations are licensed under the identical terms.

Open peer reviewers: Paulina Carriba, Cardiff University, UK; Karthik Krishnamurthy, Thomas Jefferson University, USA.

Additional files:

Additional Figure 1: Running distance measurement.

Additional Figure 2: Effects of voluntary exercise on recognition ability in 5- and 9-month-old APP/PS1 mice with or without AQP4.

Additional Figure 3: Effects of voluntary exercise on glymphatic transport in 5- and 9-month-old APP/PS1 mice with or without AQP4.

Additional Figure 4: Effects of voluntary exercise on brain A β levels in 5- and 9-month-old APP/PS1 mice with or without AQP4.

Additional Figure 5: Effects of voluntary exercise on reactive gliosis and inflammatory factor levels in the frontal cortex of 5- and 9-month-old APP/PS1 mice with or without AQP4.

Additional Figure 6: Immunofluorescence staining showing the effects of voluntary exercise on AQP4 expression and polarity in 5- and 9-month-old APP/PS1 mice.

Additional Figure 7: Effects of voluntary exercise on synapsin I and PSD95 expression in the hippocampus of 5- and 9-month-old APP/PS1 mice with or without AQP4.

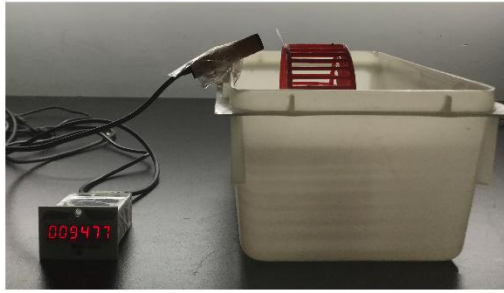
Additional file 1: Open peer review reports 1 and 2.

References

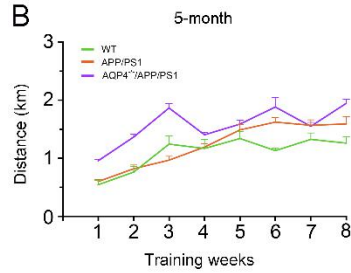
- Acosta C, Anderson HD, Anderson CM (2017) Astrocyte dysfunction in Alzheimer disease. *J Neurosci Res* 95:2430-2447.
- Adlard PA, Perreau VM, Pop V, Cotman CW (2005) Voluntary exercise decreases amyloid load in a transgenic model of Alzheimer's disease. *J Neurosci* 25:4217-4221.
- Bartolotti N, Segura L, Lazarov O (2016) Diminished CRE-induced plasticity is linked to memory deficits in familial Alzheimer's disease mice. *J Alzheimers Dis* 50:477-489.
- Blondell SJ, Hammersley-Mather R, Veerman JL (2014) Does physical activity prevent cognitive decline and dementia? A systematic review and meta-analysis of longitudinal studies. *BMC Public Health* 14:510.
- Burfeind KG, Murchison CF, Westaway SK, Simon MJ, Erten-Lyons D, Kaye JA, Quinn JF, Iliff JJ (2017) The effects of noncoding aquaporin-4 single-nucleotide polymorphisms on cognition and functional progression of Alzheimer's disease. *Alzheimers Dement (N Y)* 3:348-359.
- Caselli RJ, Beach TG, Knopman DS, Graff-Radford NR (2017) Alzheimer disease: scientific breakthroughs and translational challenges. *Mayo Clin Proc* 92:978-994.

- Chao F, Jiang L, Zhang Y, Zhou C, Zhang L, Tang J, Liang X, Qi Y, Zhu Y, Ma J, Tang Y (2018) Stereological investigation of the effects of treadmill running exercise on the hippocampal neurons in middle-aged APP/PS1 transgenic mice. *J Alzheimers Dis* 63:689-703.
- Chao MV (2003) Neurotrophins and their receptors: a convergence point for many signalling pathways. *Nat Rev Neurosci* 4:299-309.
- Da Mesquita S, Louveau A, Vaccari A, Smirnov I, Cornelison RC, Kingsmore KM, Contarino C, Onengut-Gumus S, Farber E, Raper D, Viar KE, Powell RD, Baker W, Dabhi N, Bai R, Cao R, Hu S, Rich SS, Munson JM, Lopes MB, et al. (2018) Functional aspects of meningeal lymphatics in ageing and Alzheimer's disease. *Nature* 560:185-191.
- de Oliveira Silva F, Ferreira JV, Plácido J, Sant'Anna P, Araújo J, Marinho V, Laks J, Camaz Deslandes A (2019) Three months of multimodal training contributes to mobility and executive function in elderly individuals with mild cognitive impairment, but not in those with Alzheimer's disease: A randomized controlled trial. *Maturitas* 126:28-33.
- Duman RS, Monteggia LM (2006) A neurotrophic model for stress-related mood disorders. *Biol Psychiatry* 59:1116-1127.
- Fan Y, Zhang J, Sun XL, Gao L, Zeng XN, Ding JH, Cao C, Niu L, Hu G (2005) Sex- and region-specific alterations of basal amino acid and monoamine metabolism in the brain of aquaporin-4 knockout mice. *J Neurosci Res* 82:458-464.
- Feng W, Zhang Y, Wang Z, Xu H, Wu T, Marshall C, Gao J, Xiao M (2020) Microglia prevent beta-amyloid plaque formation in the early stage of an Alzheimer's disease mouse model with suppression of glymphatic clearance. *Alzheimers Res Ther* 12:125.
- Ferrer I, Krupinski J, Goutan E, Marti E, Ambrosio S, Arenas E (2001) Brain-derived neurotrophic factor reduces cortical cell death by ischemia after middle cerebral artery occlusion in the rat. *Acta Neuropathol* 101:229-238.
- Forbes D, Thieszen EJ, Blake CM, Forbes SC, Forbes S (2013) Exercise programs for people with dementia. *Cochrane Database Syst Rev*:Cd006489.
- Francis N, Robison LS, Popescu DL, Michaelos M, Hatfield J, Xu F, Zhu X, Davis J, Anderson ME, Anderson BJ, Van Nostrand WE, Robinson JK (2020) Voluntary wheel running reduces amyloid- β 42 and rescues behavior in aged Tg2576 mouse model of Alzheimer's disease. *J Alzheimers Dis* 73:359-374.
- Goulay R, Mena Romo L, Hol EM, Dijkhuizen RM (2020) From stroke to dementia: a comprehensive review exposing tight interactions between stroke and amyloid- β formation. *Transl Stroke Res* 11:601-614.
- He XF, Liu DX, Zhang Q, Liang FY, Dai GY, Zeng JS, Pei Z, Xu GQ, Lan Y (2017) Voluntary exercise promotes glymphatic clearance of amyloid beta and reduces the activation of astrocytes and microglia in aged mice. *Front Mol Neurosci* 10:144.
- Hoshi A, Tsunoda A, Tada M, Nishizawa M, Ugawa Y, Kakita A (2017) Expression of aquaporin 1 and aquaporin 4 in the temporal neocortex of patients with Parkinson's disease. *Brain Pathol* 27:160-168.
- Hoshi A, Yamamoto T, Shimizu K, Ugawa Y, Nishizawa M, Takahashi H, Kakita A (2012) Characteristics of aquaporin expression surrounding senile plaques and cerebral amyloid angiopathy in Alzheimer disease. *J Neuropathol Exp Neurol* 71:750-759.
- Iliff JJ, Chen MJ, Plog BA, Zeppenfeld DM, Soltero M, Yang L, Singh I, Deane R, Nedergaard M (2014) Impairment of glymphatic pathway function promotes tau pathology after traumatic brain injury. *J Neurosci* 34:16180-16193.
- Iliff JJ, Wang M, Liao Y, Plogg BA, Peng W, Gundersen GA, Benveniste H, Vates GE, Deane R, Goldman SA, Nagelhus EA, Nedergaard M (2012) A paravascular pathway facilitates CSF flow through the brain parenchyma and the clearance of interstitial solutes, including amyloid β . *Sci Transl Med* 4:147ra111.
- Jahangiri Z, Gholamzad Z, Hosseini M (2019) Neuroprotective effects of exercise in rodent models of memory deficit and Alzheimer's. *Metab Brain Dis* 34:21-37.
- Ke HC, Huang HJ, Liang KC, Hsieh-Li HM (2011) Selective improvement of cognitive function in adult and aged APP/PS1 transgenic mice by continuous non-shock treadmill exercise. *Brain Res* 1403:1-11.
- Kim BY, Lee SH, Graham PL, Angelucci F, Lucia A, Pareja-Galeano H, Leyhe T, Turana Y, Lee IR, Yoon JH, Shin JJ (2017) Peripheral brain-derived neurotrophic factor levels in Alzheimer's disease and mild cognitive impairment: a comprehensive systematic review and meta-analysis. *Mol Neurobiol* 54:7297-7311.
- Kress BT, Iliff JJ, Xia M, Wang M, Wei HS, Zeppenfeld D, Xie L, Kang H, Xu Q, Liew JA, Plog BA, Ding F, Deane R, Nedergaard M (2014) Impairment of paravascular clearance pathways in the aging brain. *Ann Neurol* 76:845-861.
- Larson EB, Wang L, Bowen JD, McCormick WC, Teri L, Crane P, Kukull W (2006) Exercise is associated with reduced risk for incident dementia among persons 65 years of age and older. *Ann Intern Med* 144:73-81.
- Law CK, Lam FM, Chung RC, Pang MY (2020) Physical exercise attenuates cognitive decline and reduces behavioural problems in people with mild cognitive impairment and dementia: a systematic review. *J Physiother* 66:9-18.
- Law LL, Barnett F, Yu MK, Gray MA (2014) Effects of functional tasks exercise on older adults with cognitive impairment at risk of Alzheimer's disease: a randomised controlled trial. *Age Ageing* 43:813-820.
- Li Z, Ip B, Mok VCT, Ko H (2021) Neurovascular ageing: transcriptomic readout and implications on therapeutic targeting in Alzheimer's disease. *Neural Regen Res* 16:2411-2412.
- Liu PZ, Nusslock R (2018) Exercise-Mediated Neurogenesis in the Hippocampus via BDNF. *Front Neurosci* 12:52.
- Liu W, Wang X, O'Connor M, Wang G, Han F (2020) Brain-derived neurotrophic factor and its potential therapeutic role in stroke comorbidities. *Neural Plast* 2020:1969482.
- Lopatoglu Cabezas I, Herrera Batista A, Pentón Rol G (2014) The role of glial cells in Alzheimer disease: potential therapeutic implications. *Neurologia* 29:305-309.
- Lueptow LM (2017) Novel object recognition test for the investigation of learning and memory in mice. *J Vis Exp*:55718.
- Manna I, De Benedittis S, Iaccino E, Quattrone A, Quattrone A (2021) Diagnostic and therapeutic potential of exosomal miRNAs in Alzheimer's disease. *Neural Regen Res* 16:2217-2218.
- Martiniowik K, Manji H, Lu B (2007) New insights into BDNF function in depression and anxiety. *Nat Neurosci* 10:1089-1093.
- Mestre H, Du T, Sweeney AM, Liu G, Samson AJ, Peng W, Mortensen KN, Stæger FF, Bork PAR, Bashford L, Toro ER, Tithof J, Kelley DH, Thomas JH, Hjorth PG, Martens EA, Mehta RI, Solis O, Blinder P, Kleinfeld D, et al. (2020) Cerebrospinal fluid influx drives acute ischemic tissue swelling. *Science* 367:eaax7171.
- Mestre H, Hablitz LM, Xavier AL, Feng W, Zou W, Pu T, Monai H, Murlidharan G, Castellanos Rivera RM, Simon MJ, Pike MM, Plá V, Du T, Kress BT, Wang X, Plog BA, Thrane AS, Lundgaard I, Abe Y, Yasui M, et al. (2018) Aquaporin-4-dependent glymphatic solute transport in the rodent brain. *Elife* 7:e40070.
- Misawa T, Arima K, Mizusawa H, Satoh J (2008) Close association of water channel AQP1 with amyloid-beta deposition in Alzheimer disease brains. *Acta Neuropathol* 116:247-260.
- Moftakhar P, Lynch MD, Pomakian JL, Vinters HV (2010) Aquaporin expression in the brains of patients with or without cerebral amyloid angiopathy. *J Neuropathol Exp Neurol* 69:1201-1209.
- Nedergaard M, Goldman SA (2016) Brain drain. *Sci Am* 314:44-49.
- Nikolenko VN, Oganessian MV, Vovkogan AD, Nikitina AT, Sozonova EA, Kudryashova VA, Rizaeva NA, Cabezas R, Avila-Rodriguez M, Neganova ME, Mikhaleva LM, Bachurin SO, Somasundaram SG, Kirkland CE, Tarasov VV, Aliev G (2020) Current understanding of central nervous system drainage systems: implications in the context of neurodegenerative diseases. *Curr Neuropharmacol* 18:1054-1063.
- Park J, Madan M, Chigurupati S, Baek SH, Cho Y, Mughal MR, Yu A, Chan SL, Pattisapu JV, Mattson MP, Jo DG (2021) Neuronal aquaporin 1 inhibits amyloidogenesis by suppressing the interaction between beta-secretase and amyloid precursor protein. *J Gerontol A Biol Sci Med Sci* 76:23-31.
- Paxinos G, Franklin KB (2013) *The Mouse Brain in Stereotaxic Coordinates*. San Diego: Elsevier.
- Peng S, Wu J, Mufson EJ, Fahnestock M (2005) Precursor form of brain-derived neurotrophic factor and mature brain-derived neurotrophic factor are decreased in the pre-clinical stages of Alzheimer's disease. *J Neurochem* 93:1412-1421.
- Peng W, Acharyar TM, Li B, Liao Y, Mestre H, Hitomi E, Regan S, Kasper T, Peng S, Ding F, Benveniste H, Nedergaard M, Deane R (2016) Suppression of glymphatic fluid transport in a mouse model of Alzheimer's disease. *Neurobiol Dis* 93:215-225.
- Percie du Sert N, Hurst V, Ahluwalia A, Alam S, Avey MT, Baker M, Browne WJ, Clark A, Cuthill IC, Dirnagl U, Emerson M, Garner P, Holgate ST, Howells DW, Karp NA, Lázic SE, Lidster K, MacCallum CJ, Macleod RM, Pearl EJ, et al. (2020) The ARRIVE guidelines 2.0: Updated guidelines for reporting animal research. *PLoS Biol* 18:e3000410.
- Pérez E, Barrachina M, Rodríguez A, Torrejón-Escribano B, Boada M, Hernández I, Sánchez M, Ferrer I (2007) Aquaporin expression in the cerebral cortex is increased at early stages of Alzheimer disease. *Brain Res* 1128:164-174.
- Piantino J, Lim MM, Wedger CD, Iliff J (2019) Linking traumatic brain injury, sleep disruption and post-traumatic headache: a potential role for glymphatic pathway dysfunction. *Curr Pain Headache Rep* 23:62.
- Poo MM (2001) Neurotrophins as synaptic modulators. *Nat Rev Neurosci* 2:24-32.
- Poon WW, Blurton-Jones M, Tu CH, Feinberg LM, Chabrier MA, Harris JW, Jeon NL, Cotman CW (2011) Beta-amyloid impairs axonal BDNF retrograde trafficking. *Neurobiol Aging* 32:821-833.
- Quan H, Koltai E, Suzuki K, Aguiar AS, Jr, Pinho R, Boldogh I, Berkes I, Radak Z (2020) Exercise, redox system and neurodegenerative diseases. *Biochim Biophys Acta Mol Basis Dis* 1866:165778.
- Querfurth HW, LaFerla FM (2010) Alzheimer's disease. *N Engl J Med* 362:329-344.
- Rasmussen MK, Mestre H, Nedergaard M (2018) The glymphatic pathway in neurological disorders. *Lancet Neurol* 17:1016-1024.
- Reeves BC, Karim JK, Kundishora AJ, Mestre H, Cerci HM, Matouk C, Alper SL, Lundgaard I, Nedergaard M, Kahle KT (2020) Glymphatic system impairment in Alzheimer's disease and idiopathic normal pressure hydrocephalus. *Trends Mol Med* 26:285-295.
- Richards M, Hardy R, Wadsworth ME (2003) Does active leisure protect cognition? Evidence from a national birth cohort. *Soc Sci Med* 56:785-792.
- Robison LS, Popescu DL, Anderson ME, Francis N, Hatfield J, Sullivan JK, Beigelman SI, Xu F, Anderson BJ, Van Nostrand WE, Robinson JK (2019) Long-term voluntary wheel running does not alter vascular amyloid burden but reduces neuroinflammation in the Tg-SwDI mouse model of cerebral amyloid angiopathy. *J Neuroinflammation* 16:144.
- Rodríguez A, Pérez-Gracia E, Espinosa JC, Pumarola M, Torres JM, Ferrer I (2006) Increased expression of water channel aquaporin 1 and aquaporin 4 in Creutzfeldt-Jakob disease and in bovine spongiform encephalopathy-infected bovine-PrP transgenic mice. *Acta Neuropathol* 112:573-585.
- Sadashima S, Honda H, Suzuki SO, Shijo M, Aishima S, Kai K, Aira J, Iwaki T (2004) Accumulation of astrocytic aquaporin 4 and aquaporin 1 in prion protein plaques. *J Neuropathol Exp Neurol* 79:419-429.
- Satoh J, Tabunoki H, Yamamura T, Arima K, Konno H (2007) Human astrocytes express aquaporin-1 and aquaporin-4 in vitro and in vivo. *Neuropathology* 27:245-256.
- Taoka T, Masutani Y, Kawai H, Nakane T, Matsuoka K, Yasuno F, Kishimoto T, Naganawa S (2017) Evaluation of glymphatic system activity with the diffusion MR technique: diffusion tensor image analysis along the perivascular space (DTI-ALPS) in Alzheimer's disease cases. *Jpn J Radiol* 35:172-178.
- Tarasoff-Conway JM, Carare RO, Osorio RS, Godzik L, Butler T, Fieremans E, Axel L, Rusinek H, Nicholson C, Zlokovic BV, Frangione B, Blennow K, Ménard J, Zetterberg H, Wisniewski T, de Leon MJ (2015) Clearance systems in the brain-implications for Alzheimer disease. *Nat Rev Neurosci* 11:457-470.
- Trinchese F, Liu S, Battaglia F, Walter S, Mathews PM, Arancio O (2004) Progressive age-related development of Alzheimer-like pathology in APP/PS1 mice. *Ann Neurol* 55:801-814.
- Valenza M, Facchinetti R, Steardo L, Scuderi C (2019) Altered waste disposal system in aging and Alzheimer's disease: focus on astrocytic aquaporin-4. *Front Pharmacol* 10:1656.
- Vaynman S, Ying Z, Gómez-Pinilla F (2004) Exercise induces BDNF and synapsin I to specific hippocampal subfields. *J Neurosci Res* 76:356-362.
- von Holstein-Rathlou S, Petersen NC, Nedergaard M (2018) Voluntary running enhances glymphatic influx in awake behaving, young mice. *Neurosci Lett* 662:253-258.
- Wang L, Zhang Y, Zhao Y, Marshall C, Wu T, Xiao M (2019) Deep cervical lymph node ligation aggravates AD-like pathology of APP/PS1 mice. *Brain Pathol* 29:176-192.
- Wang Q, Xu Z, Tang J, Sun J, Gao J, Wu T, Xiao M (2013) Voluntary exercise counteracts A β 25-35-induced memory impairment in mice. *Behav Brain Res* 256:618-625.
- Wolf SA, Kronenberg G, Lehmann K, Blankenship A, Overall R, Staufienbiel M, Kempermann G (2006) Cognitive and physical activity differentially modulate disease progression in the amyloid precursor protein (APP)-23 model of Alzheimer's disease. *Biol Psychiatry* 60:1314-1323.
- Xia J, Li B, Yin L, Zhao N, Yan Q, Xu B (2019) Treadmill exercise decreases β -amyloid burden in APP/PS1 transgenic mice involving regulation of the unfolded protein response. *Neurosci Lett* 703:125-131.
- Xu Z, Xiao N, Chen Y, Huang H, Marshall C, Gao J, Cai Z, Wu T, Hu G, Xiao M (2015) Deletion of aquaporin-4 in APP/PS1 mice exacerbates brain A β accumulation and memory deficits. *Mol Neurodegener* 10:58.
- Xu ZQ, Zhang LQ, Wang Q, Marshall C, Xiao N, Gao JY, Wu T, Ding J, Hu G, Xiao M (2013) Aerobic exercise combined with antioxidant treatment does not counteract moderate- or mid-stage Alzheimer-like pathophysiology of APP/PS1 mice. *CNS Neurosci Ther* 19:795-803.
- Yang J, Lunde LK, Nuntagij P, Oguchi T, Camassa LM, Nilsson LN, Lannfelt L, Xu Y, Amiry-Moghaddam M, Ottersen OP, Torp R (2011) Loss of astrocyte polarization in the tg-ArcSwe mouse model of Alzheimer's disease. *J Alzheimers Dis* 27:711-722.
- Zeng B, Zhao G, Liu HL (2020) The differential effect of treadmill exercise intensity on hippocampal soluble a β and lipid metabolism in APP/PS1 mice. *Neuroscience* 430:73-81.
- Zeppenfeld DM, Simon M, Haswell JD, D'Abreo D, Murchison C, Quinn JF, Grafe MR, Woltjer RL, Kaye J, Iliff JJ (2017) Association of perivascular localization of aquaporin-4 with cognition and Alzheimer disease in aging brains. *JAMA Neurol* 74:91-99.
- Zhang X, He Q, Huang T, Zhao N, Liang F, Xu B, Chen X, Li T, Bi J (2019) Treadmill exercise decreases a β deposition and counteracts cognitive decline in APP/PS1 Mice, Possibly Via Hippocampal Microglia Modifications. *Front Aging Neurosci* 11:78.
- Zhang Y, Li C, Zou L, Liu X, Song W (2018) The effects of mind-body exercise on cognitive performance in elderly: a systematic review and meta-analysis. *Int J Environ Res Public Health* 15:2791.

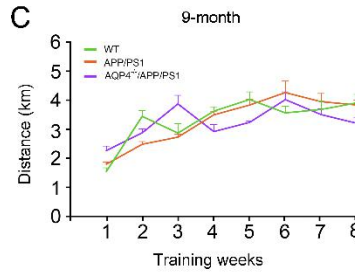
A



B

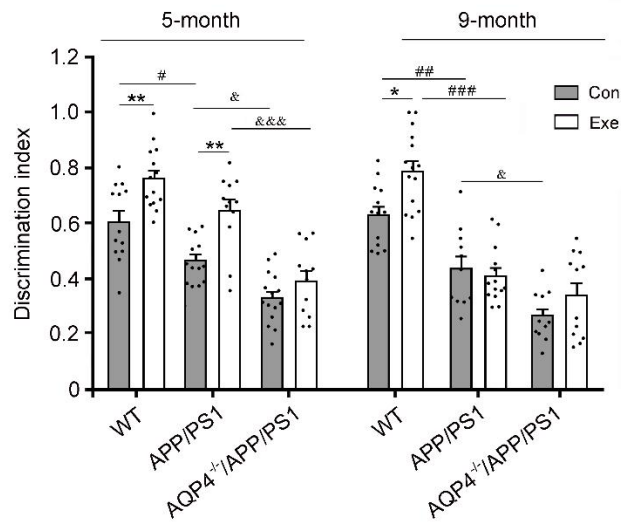


C



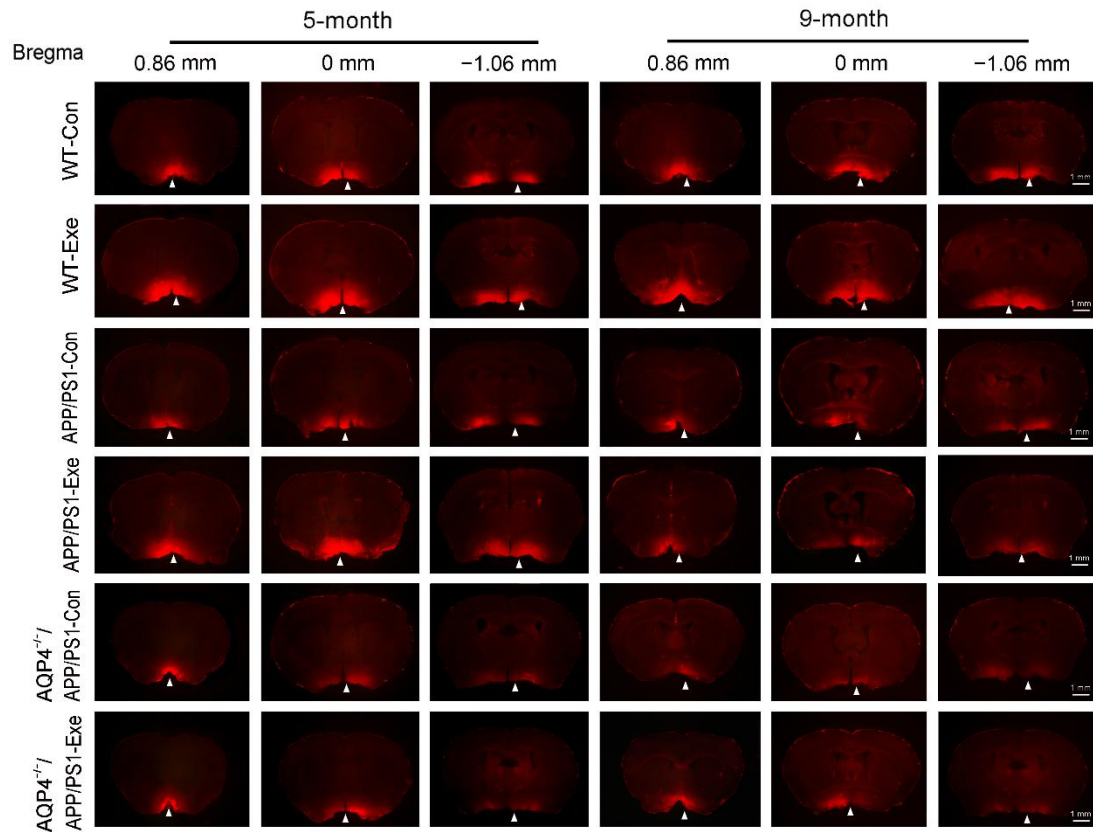
Additional Figure 1 Running distance measurement.

(A) The pedometer showing the number of laps of a mouse had run in a voluntary exercise. (B) The exercise distance of one mouse per group was measured randomly. With the increase of exercise weeks, the distance of voluntary exercise generally increased (5 months: $F_{(7, 96)} = 34.12$, $P < 0.0001$; 9 months: $F_{(7, 96)} = 26.91$, $P < 0.0001$). Moreover, the performance of the 9-month groups ($F_{(2, 96)} = 0.3797$, $P = 0.6851$) was better than that of the 5-month group (genotype effect: $F_{(2, 96)} = 55.69$, $P < 0.0001$). Data from 5 days in a week are expressed as mean \pm SEM, and were analyzed by the two-way factor analysis of variance with Tukey's post hoc test. APP/PS1: Amyloid precursor protein/presenilin-1 transgenic mice; AQP4^{-/-}/APP/PS1: aquaporin 4 gene knockout and amyloid precursor protein/presenilin-1 transgenic mice; WT: wild-type mice.



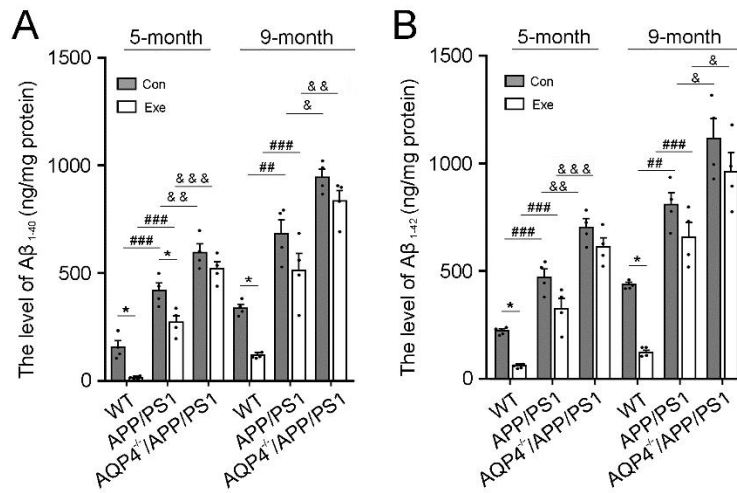
Additional Figure 2 Effects of voluntary exercise on recognition ability in 5- and 9-month-old APP/PS1 mice with or without AQP4.

The discrimination index in the novel object recognition task was calculated by the time spent exploring the novel object divided by the total time spent exploring both objects. Data represent mean \pm SEM from 12-13 mice per group and were analyzed by the two-way analysis of variance with Tukey's post hoc test. * $P < 0.05$, vs. Con group; # $P < 0.05$, ## $P < 0.01$, ### $P < 0.001$, vs. WT group; & $P < 0.05$, vs. APP/PS1 group. APP/PS1: Amyloid precursor protein/presenilin-1 transgenic mice; AQP4^{+/}/APP/PS1: aquaporin 4 gene knockout and amyloid precursor protein/presenilin-1 transgenic mice; Con: sedentary group; Exe: exercise group; WT: wild-type mice.



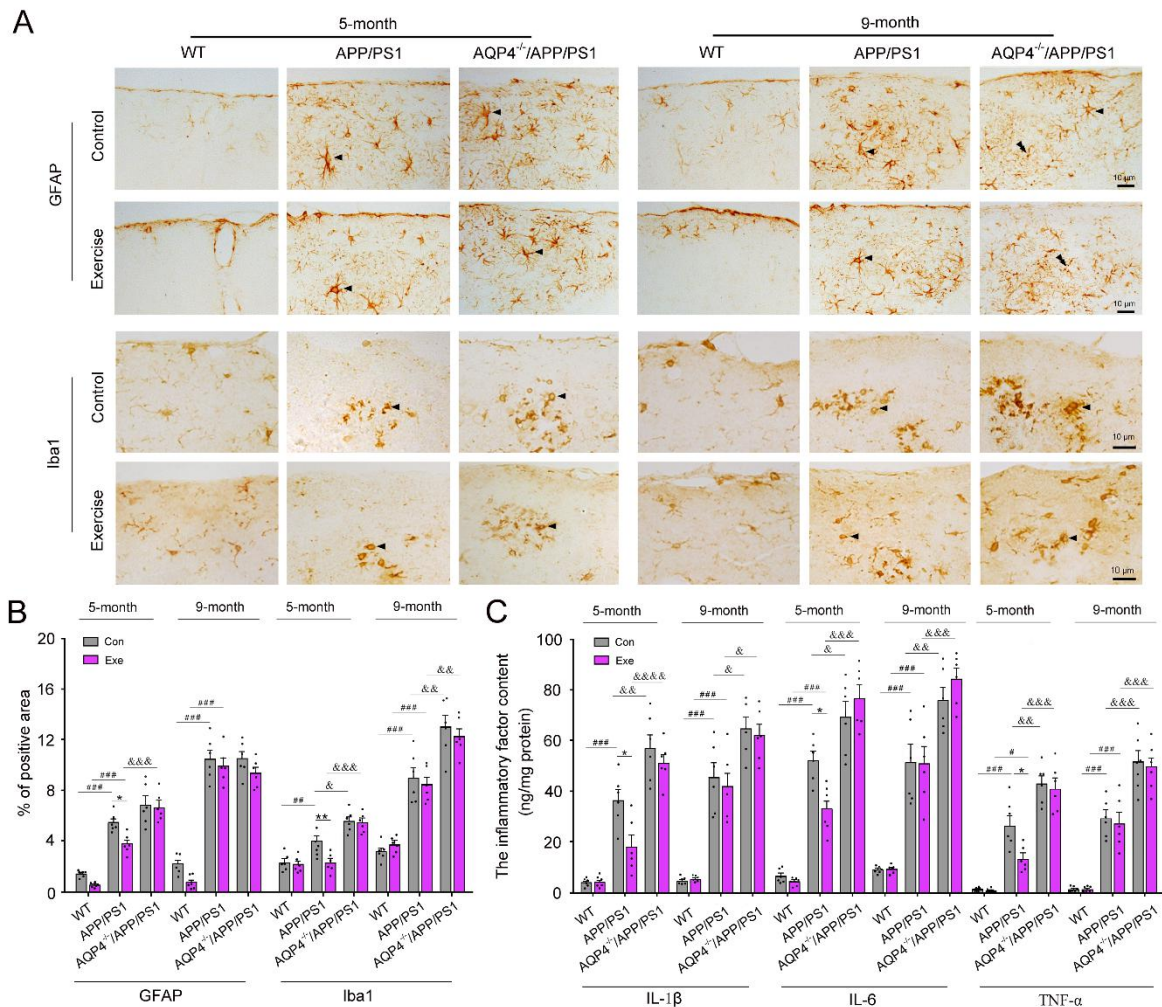
Additional Figure 3 Effects of voluntary exercise on glymphatic transport in 5- and 9-month-old APP/PS1 mice with or without AQP4.

Representative images of coronal brain sections of each group at bregma -0.86, 0 and 1.06 mm showing TR-d3 influx (arrowheads) into the brain at 40 minutes after cisterna magna injection. Exercise improved penetration of TR-d3 into the brain parenchyma in the 5- and 9-month-old WT mice and 5-month-old APP/PS1 mice, but not in the 9-month-old APP/PS1 mice and 5- and 9-month-old AQP4^{-/-}/APP/PS1 mice. Scale bars: 1 mm. APP/PS1: Amyloid precursor protein/presenilin-1 transgenic mice; AQP4^{-/-}/APP/PS1: aquaporin 4 gene knockout and amyloid precursor protein/presenilin-1 transgenic mice; Con: sedentary control group; Exe: Exercise group; TR-d3: Texas red-dextran-3; WT: wild-type mice.



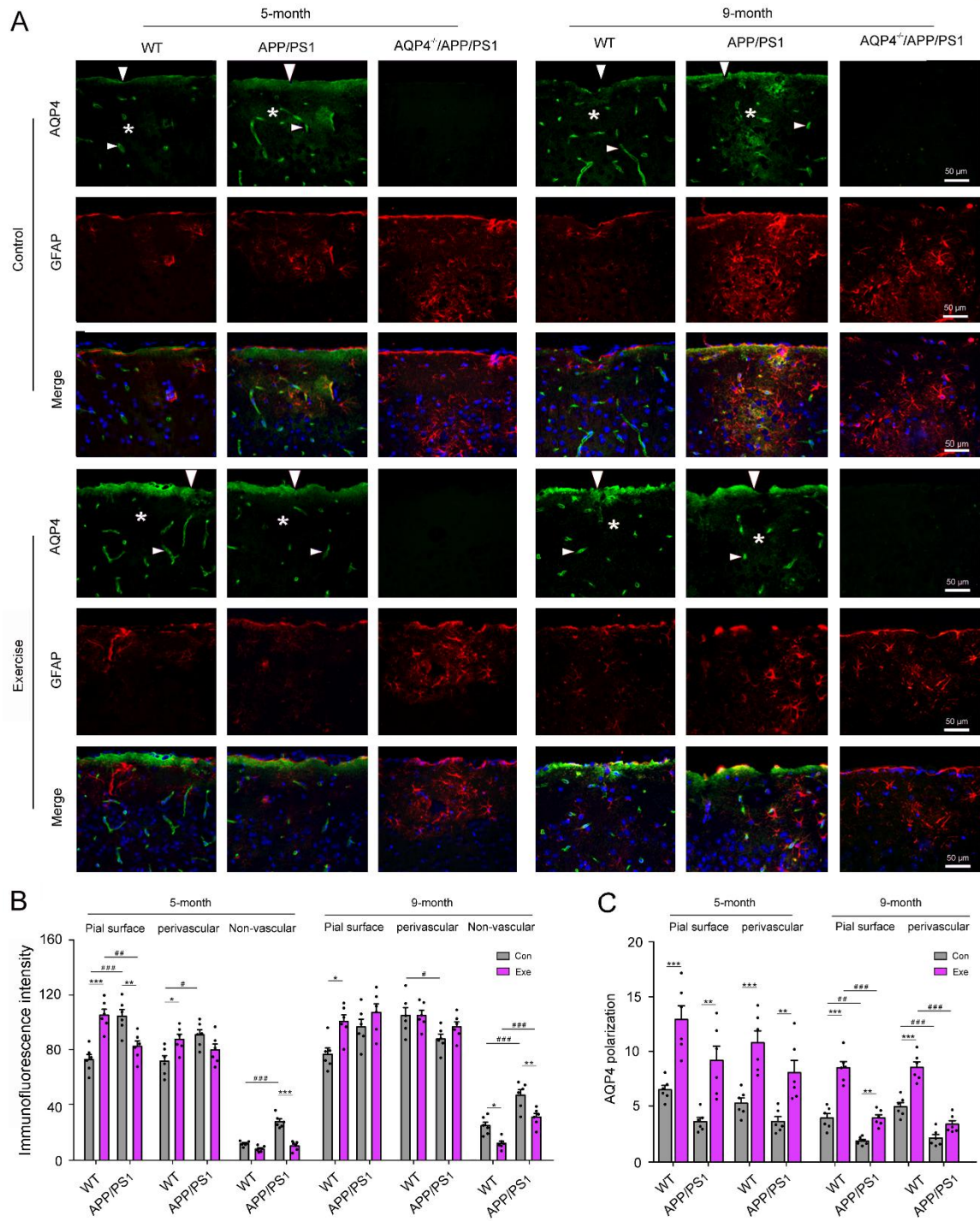
Additional Figure 4 Effects of voluntary exercise on brain Aβ levels in 5- and 9-month-old APP/PS1 mice with or without AQP4.

(A, B) ELISA analysis of the concentrations of Aβ₁₋₄₀ (A) and Aβ₁₋₄₂ (B) in the frontal cortex, respectively. Data are represented mean ± SEM from three independent experiments and four mice per group and were analyzed by the two-way analysis of variance with Tukey's post hoc test. **P* < 0.05, vs. Con group; ##*P* < 0.01, ###*P* < 0.001, vs. WT group; &*P* < 0.05, &&*P* < 0.01, &&&*P* < 0.001, vs. APP/PS1 group. Aβ₁₋₄₀: Amyloid beta peptide 1-40; Aβ₁₋₄₂: amyloid beta peptide 1-42; APP/PS1: amyloid precursor protein/presenilin-1 transgenic mice; AQP4^{-/-}/APP/PS1: aquaporin 4 gene knockout and amyloid precursor protein/presenilin-1 transgenic mice; Con: sedentary group; Exe: exercise group; WT: wild-type mice.



Additional Figure 5 Effects of voluntary exercise on reactive gliosis and inflammatory factor levels in the frontal cortex of 5- and 9-month-old APP/PS1 mice with or without AQP4.

(A) Immunohistochemical staining for GFAP and Iba1 in the frontal cortex. Exercise reduced activation of GFAP-positive astrocytes (arrowheads) and Iba1-positive microglia (arrowheads) in the 5-month-old APP/PS1 mice, but not in the 9-month-old APP/PS1 mice and 5- and 9-month-old AQP4^{-/-}/APP/PS1 mice. Scale bars: 10 μm. (B) Quantification of the percentage of GFAP and Iba1 positive area in the frontal cortex. (C) ELISA analysis of the levels of inflammatory factors including IL-1β, IL-6 and TNF-α in the frontal cortex. Data in B are represented mean ± SEM from five sections per mouse and four mice per group and data in C are represented mean ± SEM from three independent experiments and six mice per group. All data were analyzed by the two-way analysis of variance with Tukey's post hoc test. **P* < 0.05, vs. Con group; #*P* < 0.05, ##*P* < 0.01, ###*P* < 0.001, vs. WT group; &*P* < 0.05, &&*P* < 0.01, &&&*P* < 0.001, vs. APP/PS1 group. APP/PS1: Amyloid precursor protein/presenilin-1 transgenic mice; AQP4^{-/-}/APP/PS1: aquaporin 4 gene knockout and amyloid precursor protein/presenilin-1 transgenic mice; Con: sedentary group; Exe: exercise group; IL-1β: interleukin 1 beta; IL-6: interleukin 6; TNF-α: tumor necrosis factor-α; WT: wild-type mice.

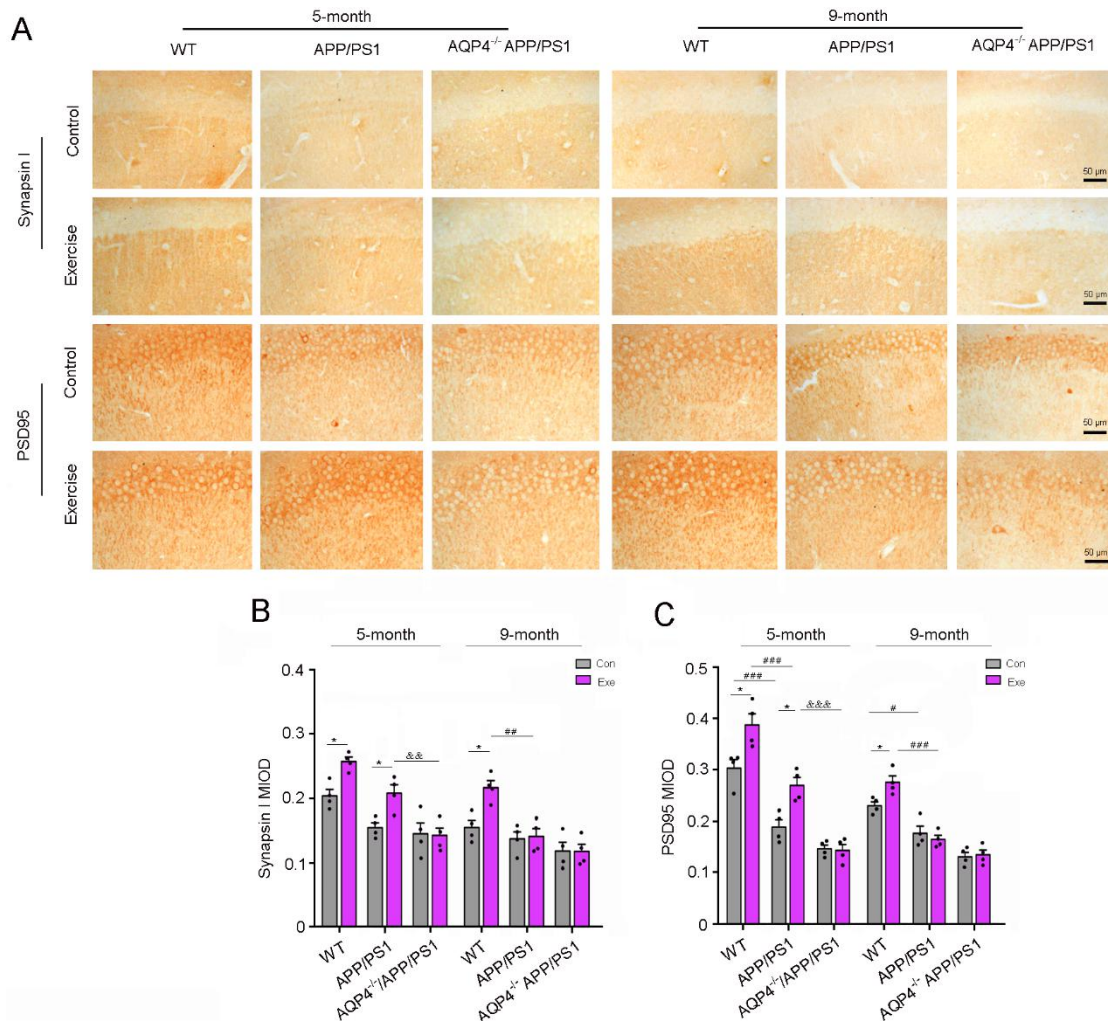


Additional Figure 6 Immunofluorescence staining showing the effects of voluntary exercise on AQP4 expression and polarity in 5- and 9-month-old APP/PS1 mice.

(A) AQP4 (green, Alexa Flour 488) and GFAP (red, Alexa Flour 555) double immunofluorescence in the frontal cortex. Immunofluorescence intensity of AQP4 was specifically located at the regions immediately abutting pia maters (large arrowheads) and microvessels (small arrowheads) in WT mice. Exercise ameliorated abnormal expression of AQP4 in the parenchymal domains (stars) of APP/PS1 mice at 5 months old, but not at 9 months old. Scale bars: 50 μ m. (B) Quantitative analyses of immunofluorescence intensity of AQP4 at the regions immediately abutting pia maters and microvessels as well as correspondingly adjacent parenchymal domains. (C) Quantitative analyses of



AQP4 polarization abutting pia mater and microvessels. Data are represented mean \pm SEM from four sections (16-20 microvessels) per mouse and six mice per group and were analyzed by the two-way analysis of variance with Tukey's post hoc test. $*P < 0.05$, $**P < 0.01$, $***P < 0.001$, vs. Con group; $\#P < 0.05$, $###P < 0.001$, vs. WT group. APP/PS1: Amyloid precursor protein/presenilin-1 transgenic mice; AQP4^{-/-}/APP/PS1: aquaporin 4 gene knockout and amyloid precursor protein/presenilin-1 transgenic mice; Con: sedentary control group; Exe: exercise group; GFAP: glial fibrillary acidic protein; WT: wild-type mice.



Additional Figure 7 Effect of voluntary exercise on synapsin I and PSD95 expression in the hippocampus of 5- and 9-month-old APP/PS1 mice with or without AQP4.

(A) Immunohistochemical staining for synapsin I and PSD95 in the hippocampus. Scale bars: 50 μ m.

(B, C) Quantification of synapsin I (B) and PSD95 (C) immunoreactive intensity in the hippocampus, respectively. Exercise enhanced the synapsin I and PSD95 expression levels in the 5-month-old APP/PS1 mice, but not in the 9-month-old APP/PS1 mice and 5- and 9-month-old AQP4^{-/-}/APP/PS1 mice. Data are represented mean \pm SEM from four sections per mouse and four mice per group and were analyzed by the two-way analysis of variance with Tukey's post hoc test. * $P < 0.05$, vs. Con group; # $P < 0.05$, vs. WT group; & $P < 0.05$, vs. AQP4^{-/-}/APP/PS1 group. APP/PS1: Amyloid precursor protein/presenilin-1 transgenic mice; AQP4^{-/-}/APP/PS1: aquaporin 4 gene knockout and amyloid precursor protein/presenilin-1 transgenic mice; Con: sedentary group; Exe: exercise group; PSD95: postsynaptic density protein 95; WT: wild-type mice.